

Journal of Materials Chemistry B

Accepted Manuscript



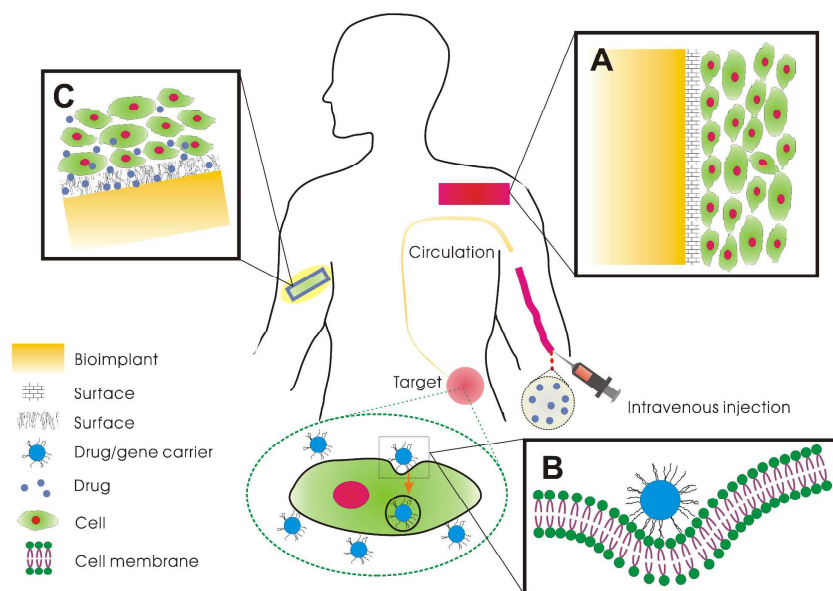
This is an *Accepted Manuscript*, which has been through the Royal Society of Chemistry peer review process and has been accepted for publication.

Accepted Manuscripts are published online shortly after acceptance, before technical editing, formatting and proof reading. Using this free service, authors can make their results available to the community, in citable form, before we publish the edited article. We will replace this *Accepted Manuscript* with the edited and formatted *Advance Article* as soon as it is available.

You can find more information about *Accepted Manuscripts* in the [Information for Authors](#).

Please note that technical editing may introduce minor changes to the text and/or graphics, which may alter content. The journal's standard [Terms & Conditions](#) and the [Ethical guidelines](#) still apply. In no event shall the Royal Society of Chemistry be held responsible for any errors or omissions in this *Accepted Manuscript* or any consequences arising from the use of any information it contains.

Table of Content



Recent progress pertaining to the surface treatment of implantable macro-scale biomaterials as well as micro- and nano-biomaterials for disease diagnosis and drug/gene delivery is reviewed.

Engineering and functionalization of biomaterials *via* surface modification

Guosong Wu, Penghui Li, Hongqing Feng, Xuming Zhang, Paul K. Chu*

Department of Physics and Materials Science, City University of Hong Kong, Tat

Chee Avenue, Kowloon, Hong Kong, China

It is imperative to control the interactions between biomaterials and living tissues to optimize the therapeutic effects and disease diagnostics. Since most biomaterials do not have the perfect surface properties and desirable functions, surface modification plays an important role in tailoring the surface of biomaterials to allow better adaptation to the physiological surroundings and deliver the required clinical performance. This paper reviews recent progress pertaining to the surface treatment of implantable macro-scale biomaterials for orthopedic and dental applications as well as micro- and nano-biomaterials for disease diagnosis and drug/gene delivery. Recent advance in surface modification techniques encompassing adsorption, deposition, ion implantation, covalent binding, and conversion has spurred more expeditious development of new-generation biomaterials.

* Corresponding author. *E-mail: paul.chu@cityu.edu.hk (P. K. Chu)*

1. Introduction

Biomaterials are traditionally defined as materials used in medical devices but as the field evolves, biomaterials are being constantly refined both in sophistication and diversity, and presently become as important as food and drugs in modern medicine¹. Bulk biomaterials designed primarily for tissue repair and reconstruction as well as substitutes for soft and hard tissues and dental materials (Fig. 1A) require a sufficient load-bearing capability. In addition, depending on the functions and biological environment, good blood compatibility, osseo-compatibility and low toxicity are essential to biomedical implants *in vivo*. In some cases, degradability is also a desirable feature². However, unexpected degradation arising from wear and corrosion can produce micrometer- and nanometer-scale debris and metal ions that may be detrimental to human health *via* interactions with surrounding tissues to induce deleterious effects such as tissue impairment, inflammation, and ultimately implant failure³. In these cases, the surface on the biomedical implant must act as a shield to protect against undesirable degradation and provide a platform for cells to proliferate and differentiate especially in orthopedic applications.

When the size of biomaterials is reduced from the macro- to micro-nanoscale (Fig. 1B), they can be administered orally or by intravascular/intramuscular injection. The human circulatory system transports them throughout the body and micro- and nano-scale biomaterials can arrive at the targeted sites by either active or passive

targeting. Hence, biomaterials such as nanoparticles, nanocapsules, micelles, dendrimers, and so on can be selectively captured by cells and serve as carriers in drug/gene delivery, bio-sensing, bio-imaging, and photo-thermal therapy⁴. After delivery to the proper bio-environment, they interact with proteins, membranes, cells, DNA, and organelles to establish a series of nanoparticle/biological interfaces that depend on colloidal forces as well as dynamic bio-physico-chemical interactions, subsequently leading to the formation of protein coronas, particle wrapping, intracellular uptake, and bio-catalytic processes that have compatible or adverse outcome⁵. The common problems in systemic particulate delivery are renal clearance, poor targeting efficiency, and degradation by serum nucleases. Therefore, large doses are often required to improve the therapeutic effects but increased toxicity or undesirable side effects are concerns. Different from particulate drug-delivery devices, macro-scale drug delivery (MDD) devices are developed to provide spatiotemporal control of a wide range of bioactive agents including small molecules, proteins, and cells (Fig. 1C). In clinical applications, the MDD system as a reservoir of drugs is localized to the treatment site and releases the drugs in a prescribed manner in order to enhance the drug effectiveness, reduce side effects, and protect labile drugs⁶. Furthermore, drug/gene carriers as well as drugs themselves may be placed in the macro-scale device⁷. In contrast to the common medical implants shown in Fig. 1A, a different strategy is adopted to design MDD systems. The surface is not only a barrier to resist corrosion or wear, but also a reservoir for drugs, genes, and associated nanocarriers. This intriguing strategy constitutes a new trend

in biomaterials development and biomedical applications.

The interface between the biomaterials and physiological surroundings plays a vital role in the performance of the biomaterials. It is well known that cellular interactions with the extracellular matrix are of fundamental importance in many normal and pathological biological processes⁸. In this respect, the physical and chemical properties of materials can regulate biological responses⁹. The surface of biomaterials can be made more resistant to corrosion or wear and simultaneously more biocompatible by changing the composition and/or microstructure. Many types of bulk materials possess excellent mechanical properties but may not be compatible with biological tissues and fluids *in vivo*. After surface modification, properties such as cyto-compatibility, osseo-conductivity, and bacteria resistance can be attained selectively and controllably while the favorable bulk attributes of the materials such as strength and robustness can be preserved¹⁰. With regard to conventional nanocarriers, they may be prone to premature leakage and uncontrollable release. Surface modification can improve the stability and simultaneously endow them with special functions including specific tissue/cell type targeting, stimuli-responsive release, *in vivo* imaging for diagnosis, drug delivery monitoring, and photo-thermal treatment¹¹. All in all, surface modification is applicable to biomaterials with both the macro- and nano-scale. In this review, recent advance in surface engineering and functionalization of biomaterials, with emphasis on implantable devices, drug delivery systems, tissue engineering, and so on,

is discussed to reflect the significance and prospect.

2 Implantable macro-scale biomaterials

2.1 Biomedical titanium-based implants

Titanium and its alloys have been widely used in orthopedic and dental implants for many years because of their good mechanical properties and high corrosion resistance. However, two major complications may be encountered in clinical applications: lack of bone tissue integration and implant-centered infection. Ti-based implants are in contact with proteins, bacteria and tissue cells which play crucial roles in the success or failure of the implants¹²⁻¹⁴. Therefore, it is imperative to design Ti-based alloy surfaces to facilitate osseo-integration and mitigate adverse tissue response such as foreign body reactions and infection¹⁵. So far, many surface treatment methods have been attempted on Ti-based alloys and Fig. 2 shows four common types of modified surfaces. In region A, the surface of the Ti-based alloy is reconstructed by high-energy methods such as ion implantation and laser melting to obtain a new chemical composition or microstructure. Regions B and C denote the dense coating and porous coating on the surface of the Ti-based alloy, respectively. Region D shows the nanostructure on the surface of Ti-based alloy such as nanoflowers and nanotubes. These strategies will be discussed in details with specific examples in the following sections.

Plasma immersion ion implantation (PIII) is a process in which the samples are

surrounded by a high-density plasma and pulse-biased to a high negative potential relative to the chamber wall. Ions generated in the overlying plasma are accelerated across the plasma sheath formed around the samples and implanted into the sample surface. Because PIII is a non-line-of-sight process as opposed to conventional beam-line ion implantation, samples possessing a sophisticated shape can be treated with good conformality and uniformity¹⁶. Obviously, it is very suitable for biomaterials. For instance, nitrogen or oxygen PIII induces the formation of TiN or TiO₂ on surgical NiTi shape memory alloy to reduce leaching of deleterious Ni ions¹⁷⁻²¹. Recently, Zhao et al.²² conducted nitrogen and carbon plasma immersion ion implantation (N-PIII and C-PIII) on Ti6Al4V alloy to produce a graded surface layer composed of TiN and TiC, respectively. *In vitro* studies disclose improved cell adhesion and proliferation after PIII. Micro-CT evaluation conducted 1 to 12 weeks after surgery reveals larger average bone volume and less bone resorption on the N-PIII and C-PIII Ti alloy pins than the untreated one at every time point. The enhancement may be attributed to the good cyto-compatibility, appropriate surface roughness, and excellent corrosion resistance of the TiN and TiC structures which stimulate the response of cells and induce early bone formation. Cao et al.²³ used silver plasma immersion ion implantation (Ag-PIII) to construct an antimicrobial surface. Silver nanoparticles (Ag NPs) precipitate on and underneath the titanium surface *via* a local nucleation process in the solid solution of α -Ti (Ag). The Ag-implanted Ti samples are highly effective in inhibiting both *Staphylococcus aureus* and *Escherichia coli* while exhibiting obvious activity in promoting

proliferation of the osteoblast-like cell line MG63. The controlled antibacterial activity, low surface toxicity, and good cyto-compatibility are believed to stem from micro-galvanic effects between the Ag NPs and titanium matrix.

Coatings are important to biomedical application of Ti alloys. Calcium-phosphorus (Ca-P) coatings such as hydroxyapatite (HA) and tricalcium phosphate (TCP) are some of the most popular osteo-conductive materials and have been widely used to construct new bones and promote osteo-integration on Ti-based implants because calcium and phosphorus are two major elements in bone tissues²⁴⁻²⁸. Recently, Alghamdi et al.²⁹ utilized radio-frequency (RF) magnetron sputtering to deposit Ca-P coatings on titanium implants and investigated the implant-bone response under osteoporotic and healthy conditions. In their experiments, osteoporosis was induced in female Wistar rats by ovariectomy and sham-operated rats serving as controls. The Ca-P coatings enhanced the bone-to-implant contact compared to the untreated implants in both the osteoporotic and sham-operated groups. Osteoporosis in rats had a significant negative effect on the amount of bone close to the implants, but the usage of osteogenic Ca-P coatings had a positive effect on the bone implant interface under both the osteoporotic and sham-operated conditions. Besides the requirement of osteo-conductivity, attempts have been made to construct osteo-inductive surfaces on Ti-based implants to promote new bone formation. One of the effective methods is to incorporate or graft bone morphogenetic proteins (BMPs) on Ti alloys. Fig. 3 illustrates the preparation of

polyelectrolyte multilayered (PEM) films loaded with BMP-2 on porous titanium implants. Polyethyleneimine (PEI), poly(L-lysine) hydrobromide (PLL), and hyaluronic acid (HA) are dissolved in a buffered saline solution, followed by a dipping process for cross-linking to fabricate the multilayered PLL/HA films on the titanium samples. The PEM-coated samples are incubated in the BMP-2 solution and the amount of BMP-2 incorporated into these films is adjusted based on the cross-linking extent of the film and initial BMP-2 concentration. The osteo-inductive properties are determined from the Ti surface and the local bone formation activity is enhanced³⁰. Anodic oxidation is a traditional technique to prepare porous coatings on Ti-based alloys and Yue et al.³¹ have used it to fabricate porous TiO₂ coatings on Ti and Ti alloys (Fig. 4). Generally, when TiO₂ is exposed to UV light, electron-hole pairs are generated in the valence band to react with oxygen and atmospheric water to yield reactive oxygen species, which are capable of decomposing organic molecules including micro-organisms in contact. They applied UV light to photo-catalytically activate the anodized samples and found that the treated surfaces killed peri-operatively introduced bacteria successfully. Surface coverage by osteoblasts was not affected by photo-catalytic activation of the anodized surface but in the co-culture of osteoblasts with contaminating *Staphylococcus epidermidis*, surface coverage on the photo-catalytically-activated TiO₂-surfaces was enhanced.

Nowadays, nanotechnology is one of the hottest topics in biomaterials research and

fabrication of a nanostructured surface on biomaterials is a versatile strategy to tailor the biological properties. When a surface contains micro- and nano-scale features in a controlled fashion, the cellular and subcellular functions are modified significantly³². Zhao et al.³³ prepared hierarchical hybrid micro/nano-textured surface topographies on titanium with titania nanotubes by simple acid etching followed by anodization to mimic the hierarchical structure of bone tissues (Fig.5). The micro-texture produced by acid etching induced inconsistent osteoblast functions. Initial cell adhesion and osteo-genesis-related gene expressions were enhanced dramatically whereas the other cell behavior such as proliferation, intracellular total protein synthesis, alkaline phosphatase activity, collagen secretion, and extracellular matrix mineralization was depressed significantly. Addition of nanotubes to the micro-structured surface enhances the multiple osteoblast behavior with nearly all the aforementioned cell functions being retained or promoted. Tsukimura et al.³⁴ developed a kind of novel micro/nano hybrid topography (TiO₂ nanonodules in micro-scale pits) on titanium, which showed a higher biological capability than micro-topography. Furthermore, the effect of UV photo-functionalization could be multiplied on micro/nano hybrid titanium compared to surfaces with only micropits. Li et al.³⁵ obtained a hierarchical TiO₂ film on Ti by acid etching to produce micropits, followed by a hydrothermal treatment to generate TiO₂ nanorods. This hierarchical TiO₂ film exhibited enhanced bioactivity and bacteriostatic effect due to the more negative zeta potential. Ag PIII was performed to impregnate Ag into the TiO₂ surface and the addition of embedded Ag remarkably enhanced the antimicrobial efficiency as a result of the

Schottky contact without Ag^+ release.

It is desirable to create drug-eluting implants to deliver drugs locally to enhance osseo-integration and shorten the healing time after implantation. Nanotubes with a large surface area-to-volume ratio and controllable dimensions are good candidates for carrying and delivering drugs and anti-bacterial agents³⁶⁻³⁸. For example, Gulati et al.³⁹ fabricated titania nanotubes (TNTs) on titanium by electrochemical anodization and loaded the water-insoluble anti-inflammatory drug indomethacin. Two biodegradable and antibacterial polymers, chitosan and poly(lactic-co-glycolic acid), were formed on the drug-loaded TNTs by a simple dip-coating process. Fig. 6 shows the preparation process and SEM images of the modified titania nanotubes with the polymer films. The drug release time was successfully extended after modification and better osteoblast adhesion and cell proliferation were observed from the polymer-coated TNTs.

Strontium (Sr) is an alkaline earth metal element having a positive effect on bone homeostasis. Sr affects bone resorbing osteoclasts as well as bone forming osteoblasts in bone remodeling⁴⁰. Nanotube arrays produced on the Ti surface can not only load drugs as described above but also act as carriers for Sr. Xin et al.⁴¹ have fabricated ordered SrTiO_3 nanotube arrays on titanium with a slow Sr release rate by a hydrothermal treatment of anodized titania nanotubes. This surface architecture which combines the virtues of nanostructures and Sr release possesses

good biocompatibility and induces precipitation of hydroxyapatite from simulated body fluids (SBF). Zhao et al.⁴² fabricated strontium-loaded nanotubular (NT-Sr) structures by hydrothermal treatment of titania nanotubes. The loaded Sr amounts can be regulated by the hydrothermal treatment time in the $\text{Sr}(\text{OH})_2$ solution. Sr incorporation enhances proliferation of rat mesenchymal stem cells (MSCs) on the nanotube and promotes the spread of MSCs into a polygonal osteoblastic shape (Fig. 7). NT-Sr can significantly up-regulate the expression of the osteogenesis related genes in the absence of an extra osteogenic agent. Hence, a strontium-releasing surface with excellent osteogenic properties is very attractive clinically.

In summary, surface modification is one of the important ways to improve bone tissue integration and avoid tissue infection on Ti-based alloys in clinical applications. Many conventional techniques such as ion implantation are finding new applications in the development of biomedical Ti-based alloys. In addition, the emergence of nanotechnology provides a versatile strategy to construct bio-surfaces. For instance, nanotubes fabricated on Ti alloys not only modify the biological behavior but also act as reservoirs for drugs and other agents to perform special functions including drug delivery.

2.2 Biodegradable magnesium-based implants

Magnesium alloys constitute a new class of biodegradable metals⁴³⁻⁴⁵ which are

especially attractive in load-bearing applications. The Young's modulus ($E = 41-45$ GPa) of Mg alloys is similar to that of bones ($E = 3-20$ GPa) and therefore, the stress shielding effect can be reduced in orthopedic applications^{46,47}. Moreover, a second surgical operation to remove the implant from the patient can be obviated due to favorable biodegradation, consequently minimizing trauma in the patients and decreasing medical costs. Fig. 8 shows two viable degradation modes of Mg-based implants in cardiovascular and osteosynthetic applications. The Mg-based implants are expected to have an approximately intact initial contour in the serving period to retain the designed load-bearing capacity. After healing, faster degradation is allowed and the mechanical strength of the implant decreases gradually because the surrounding tissues can now bear the partial load⁴⁸. This scheme requires big enough corrosion resistance for controlled (reduced) degradation to ensure adequate mechanical strength and structure integrity in the healing stage. It should be noted that a relatively stable surface without producing unacceptable hydrogen evolution and other side-effects is essential to spur cell/tissue growth.

Unfortunately, *in vitro* and *in vivo* tests conducted on most commercial Mg alloys show signs of severe and rapid corrosion immediately after implantation. Moreover, commercial Mg alloys are usually designed as structural materials for industrial usage rather than biomedical application. In some cases, these alloys even contain some potentially toxic elements such as Al, RE (rare-earth), etc.⁴⁹⁻⁵³. One way is to develop new biomedical Mg alloys to cater to the actual biomedical requirements.

For example, Yuan et al. produced Mg-2.5Nd-0.2Zn-0.4Zr for next-generation vascular stent application. Compared to traditional commercial Mg alloys such as WE43 and AZ31, the new alloy not only improves the corrosion uniformity and reduces the corrosion rate, but also exhibits minimal vascular toxicity and excellent biocompatibility⁵⁴⁻⁵⁶. The other viable technique is of course surface modification. To meet clinical requirements, a temporary surface is fabricated on Mg alloys to tailor the mechanical performance, corrosion behavior, and biological properties⁵⁷.

Magnesium is one of the most active metals in the galvanic series and a magnesium alloy component is normally the active anode in contact with other common metals in aqueous solutions. The galvanic corrosion rate is determined by

$$I_g = \frac{E_c - E_a}{R_a + R_c + R_s + R_m},$$

where I_g is the galvanic current between the anode and cathode, E_c and E_a are the open circuit potentials of the cathode and anode, R_c and R_a are the cathode resistance and anode resistance, respectively, R_s is the resistance of the solution between the anode and cathode, and R_m is the metal resistance between the anode and cathode through a metallic path⁵⁸. The galvanic effect affects the effectiveness of surface modification of Mg alloys. Taking a coating as an example, the electrolyte in the biological environment can penetrate the coating *via* cracks and pores created in the coating to form galvanic cells. According to the above formula, the galvanic current can be reduced by decreasing the potential difference ($E_c - E_a$) and increasing the cathode resistance related to the coating (R_c) and electrical resistance between the

anode and cathode (R_m). Therefore, it is better to select relatively insulating coatings such as calcium-phosphorus (Ca-P) coatings and coatings prepared by microarc oxidation (MAO) for Mg alloys.

Biocompatible calcium-phosphorus (Ca-P) coatings can be prepared on Mg alloys chemically or electrochemically. Niu et al.⁵⁹ developed a chemical method to treat Mg-Nd-Zn-Zr alloys. They immersed them in 0.1 M KF for 24 h to form a MgF_2 film and then immersed them in a mixture of $NaNO_3$, $Ca(H_2PO_4)_2 \cdot H_2O$ and H_2O_2 for 24 h to obtain a brushite ($CaHPO_4 \cdot 2H_2O$) coating. The Ca-P treatment improved the corrosion resistance of the Mg-Nd-Zn-Zr alloy in Hank's solution, reduced the hemolysis rate of the Mg-Nd-Zn-Zr alloy from 48% to 0.68%, and induced no toxicity to MC3T3-E1 cells. The *in vivo* implantation experiments performed on New Zealand rabbit tibia showed that the degradation rate was reduced by the Ca-P treatment and less gas was produced from the Ca-P treated Mg-based bone plates and screws in the early stage of implantation. Xu et al.⁶⁰ prepared a porous and net-like Ca-P coating on the Mg-Mn-Zn alloy by a phosphate treatment. The Ca-P coating composed mainly of $CaHPO_4 \cdot 2H_2O$ with small amounts of Zn and Mg significantly improved the osteo-conductivity and osteo-genesis in the initial 4 weeks after operation. Song et al.⁶¹ coated AZ91D magnesium alloys with bioactive Ca-P coatings. They performed electro-deposition to obtain a coating consisting of dicalcium phosphate dihydrate ($CaHPO_4 \cdot 2H_2O$, DCPD) and β -tricalcium phosphate ($Ca_3(PO_4)_2$, β -TCP) that were the precursors of hydroxyapatite (HA,

$\text{Ca}_{10}(\text{PO}_4)_6(\text{OH})_2$. The coated sample was immersed in 1 M NaOH solution at 80 °C for 2 h and the as-deposited coating was transformed into a uniform HA coating. This HA coating retarded the biodegradation rate in stimulated body fluids significantly. Wang et al.⁶² used pulsed electro-deposition to fabricate calcium-deficient hydroxyapatite (Ca-def HA) on the Mg-Zn-Ca alloy and *in vivo* degradation of the Ca-def HA coating and magnesium alloy occurred almost simultaneously. The *in vivo* life time of the Ca-def HA coating was about 8 weeks. Degradation of the Ca-def HA coating may be attributed to the reaction with body fluids and substitution of Mg^{2+} ions in the Ca-def HA. In addition, histological and pathological examination showed that the Ca-def HA coating had good osteo-conductivity and promoted new bone formation.

Microarc oxidation (MAO), a high-voltage plasma-assisted anodic oxidation process, is a simple way to fabricate thick, porous, hard, and insulating ceramic coatings⁶³. Gu et al.⁶⁴ utilized this technique to modify the Mg-Ca (1 wt. %) alloy and controlled the thickness and pore size of the MAO coating by tuning the applied voltage. The coating comprised the MgO and Mg_2SiO_4 phases. After microarc oxidation, the long-term corrosion resistance in Hank's solution was improved and cyto-compatibility including adhesion, proliferation, and differentiation of MG63 cells were promoted. Ryu et al.⁶⁵ fabricated Ag-containing MAO coatings on the AZ31 magnesium alloy using AgNO_3 -containing electrolytes. This MAO coating not only exhibited higher corrosion resistance than the Ag-free MAO coatings, but

also showed excellent antibacterial activity of over 99.9% against two strains of bacteria, *Staphylococcus aureus* and *Escherichia coli*. Hence, it is possible to reduce the risk of bacterial infection after surgery if antimicrobial MAO coatings are used. To evaluate the *in vivo* degradation performance, Fischerauer et al.⁶⁶ implanted the MAO-modified ZX50 Mg alloys into the femoral legs of male Sprague-Dawley rats and monitored them by micro-computed tomography (μ CT) for a period of 24 weeks. As shown in Fig. 9, almost no corrosion was observed from the MAO-treated implants in the first week but in contrast, several obvious pits emerged from the untreated ZX50 implant. The MAO preserved the integrity in the first week and so degradation was significantly mitigated. Since MAO coatings can delay initial degradation after implantation, they improve fracture stabilization, minimize the burden on the post-operatively irritated surrounding tissues, and generate good bone-implant bonding.

In addition to coatings, ion implantation such as plasma immersion ion implantation (PIII) is important to the developing biodegradable Mg alloys because an ion implanted layer does not have an abrupt interface and layer delamination does not pose a serious issue. Chromium is an important element in corrosion resistant alloys such as stainless steels. However, when chromium is incorporated into magnesium by metal ion implantation, strong galvanic corrosion occurs because Cr exists in the metallic state in the implanted layer. Nevertheless, it has been found that surface degradation of pure magnesium can be retarded if oxygen ion implantation is

conducted afterwards by PIII to produce a thick surface layer consisting of chromium oxide⁶⁷. In contrast, if only oxygen PIII is conducted on Mg-Nd-Zn-Zr alloys, no significant improvement in the corrosion resistance is observed. Consequently, Wu et al.⁶⁸⁻⁷¹ have proposed an alloying principle to modify the surface by ion implantation before O-PIII. After surface alloying with Cr, Ti, Al, and Zr, the corrosion resistance of Mg-Y-RE (rare earth), Mg-Zn-Zr, and Mg-Nd-Zn-Zr is improved due to the formation of chromium oxide, titanium oxide, aluminum oxide, and zirconium oxide in the near surface, respectively. Zhao et al.⁷² have extended this principle to Mg-Ca and Mg-Sr alloys by conducting zirconium and oxygen ion implantation. The process not only enhances the corrosion resistance and *in vitro* biocompatibility significantly, but also improves the antimicrobial properties. Recently, Wu et al.⁷³ conducted C₂H₂ PIII to produce a thin layer of diamond-like carbon (DLC) film on the Mg-Nd-Zn-Zr alloy to enhance the corrosion resistance in the 0.9 % NaCl solution. The use of a metallic interlayer is a common way to enhance the adhesion between the diamond-like carbon (DLC) and Mg substrate, but the disadvantage is that the galvanic cells generated in the defects accelerate corrosion⁷⁴⁻⁷⁶. Fortunately, in ion implantation, layer adhesion is not an issue. The defects in the film can provide the possibility of eventual degradation of the bulk alloy but it should be noted that the DLC film is not fully biodegradable and remains in the human body to possibly induce adverse effects. To avoid or reduce this phenomenon, Xu et al.⁷⁷ performed carbon ion implantation using graphite in a cathodic arc source to modify pure magnesium. A composite oxide film containing amorphous carbon

was formed on the surface and as expected, the corrosion resistance in the simulated physiological environment was improved.

In brief, biodegradable Mg alloys are attractive due to their special properties such as natural biodegradability. However, many phenomena are still not well understood and more *in vitro* and *in vivo* investigations are needed. Based on current results, surface modification by means of ion implantation, coating deposition, and so on is important to the development of biodegradable Mg alloys. With the combination of modern metallurgy and advanced surface treatment technology, Mg-based alloys have large potential as next-generation materials for biodegradable biomedical implants.

2.3 Biomedical polymer-based implants

Many types of surgical implants and medical devices are made of polymeric materials such as polyethylene (PE)^{78, 79}, polytetrafluoroethylene (PTFE)^{80, 81}, poly(lactic acid) (PLA)^{82, 83}, and polyetheretherketone (PEEK)⁸⁴⁻⁸⁶. Unfortunately, biomedical application of polymers such as trauma, orthopedics, and spinal implants are hindered in many cases by the insufficient biocompatibility and poor bacteria resistance⁸⁷⁻⁸⁹. Engineering a better surface on a biopolymer is thus critical and several recent examples pertaining to surface modification are introduced as follows.

Surface modification can produce bioactive surfaces on biopolymers while

preserving the excellent bulk properties of the materials. Compared to metals and ceramics, polymers typically have lower heat resistance. Higher temperature can distort the shape and even change the chemical composition possibly leading to failure. Many physical and chemical methods require a high temperature and/or post thermal treatment and so it is critical to choose a suitable method for polymers. Electron beam deposition, a traditional low-temperature coating process, has been used to coat polyetheretherketone (PEEK) with a Ti film because Ti has good biocompatibility only surpassed by bioactive ceramics (such as hydroxyapatite and bioglass) and natural biopolymers (such as collagen and its derivatives)⁹⁰. The obtained Ti layer is dense, uniform, well crystallized and adheres strongly to the PEEK substrate. *In vitro* tests show that proliferation and differentiation of the cells (MC3T3-E1) on the coated surface are improved and *in vivo* animal tests reveal that the Ti-coated PEEK implants have a larger bone in-contact (BIC) ratio than the pure PEEK implants. Cold spraying is a solid-state deposition process conducted at a relatively low temperature by using a carrier gas to accelerate the powders to supersonic velocity prior to impacting the substrate⁹¹⁻⁹³. Lee et al.⁹⁴ applied this method to coat PEEK with a homogeneous layer of hydroxyapatite (HA) and as expected, the HA coating increased the biocompatibility *in vitro* and promoted osteo-integration *in vivo*.

In general, chemical methods are simple and do not require expensive equipment compared to physical methods. Zhao et al.⁹⁵ performed sulfonation and subsequent

water immersion to prepare a 3D porous and nanostructured network with bio-functional groups on PEEK. The porous surface promoted in-growth of soft and hard tissues into the materials and create more biological anchorage to improve the stability of the implant. Two kinds of sulfonation-treated PEEK (SPEEK) samples were prepared, namely SPEEK-W (water immersion and rinsing after sulfonation) and SPEEK-WA (SPEEK-W with further acetone rinsing) and Fig. 10 illustrates the fabrication process and morphology of the porous surface. SPEEK-WA induces pre-osteoblast functions including initial cell adhesion, proliferation, and osteogenic differentiation *in vitro* as well as substantially enhanced osseointegration and bone-implant bonding strength *in vivo* in addition to apatite-forming ability. Although SPEEK-W has a similar surface morphology and chemical composition as SPEEK-WA, its cyto-compatibility is inferior due to residual sulfuric acid. The pre-osteoblast functions, bone growth, and apatite formation on the SPEEK surfaces are affected by positive effects introduced by the 3D porous structure and SO₃H groups as well as negative ones due to the low pH environment. Actually, by employing multiple techniques, more than one function can be achieved. For instance, Yue et al.⁹⁶ used an oxygen plasma to activate polydimethylsiloxane (PDMS) and then treated it with silane bearing ethylene imine units. Hyaluronic acid (HA), an important component of the extracellular matrix playing an important role in tissue morphogenesis, wound healing, inflammation, and metastasis, was grafted covalently onto the aminated surfaces and type I collagen was conjugated onto the HA-modified PDMS to improve the cyto-compatibility in neural applications. Significantly

enhanced rat pheochromocytoma cell (PC12) growth and differentiation was observed from the bioactive PDMS and this bio-functionalized polydimethylsiloxane has potential applications in cochlear implants.

3 Functional micro- and nano-biomaterials

3.1 Polymeric nanocarriers for gene delivery

Gene therapy is an attractive approach that uses normal genes to replace or override defective genes in treating human diseases. Depending on the process of transcription that synthesizes messenger RNA from DNA and translation that synthesizes protein from messenger RNA, the nucleic acid sequence of the gene can direct the cell to synthesize a protein with a specific and correct amino acid sequence. Gene delivery is one of the critical steps in gene therapy and a good delivery system, or so-called 'vector', can provide the genes with acceptable access to the target tissues/cells and deliver them to the nucleus of the cell effectively⁹⁷. There are two major gene delivery vectors, namely viral and non-viral ones. Viral vectors have high gene transfection efficiency, but the disadvantages are immunogenicity, potential of insertional mutagenesis in the host genome, limited DNA delivery capacity, and scale of production. Non-viral vectors are promising alternatives to viral vectors because they will not elicit immune response or randomly integrate DNA into the host genome. Cationic polymers have been the major type of the non-viral vectors in recent years because they can be easily tailored and synthesized to suit specific requirements⁹⁸. The key requirements for polymeric nano-carriers from the

perspective of efficient gene delivery are: low cyto-toxicity, appropriate stability, and special functionality.

Much effort has been made to reduce the cytotoxicity of polymeric nanocarriers. For example, polyethylenimine (PEI), which contains primary, secondary, and tertiary amine groups, is one of the common cationic polymers as a non-viral gene delivery vector⁹⁹. Its transfection efficiency depends on the molecular weight and a larger higher molecular weight PEI has a higher gene transfection efficiency but also higher cytotoxicity^{100, 101}. Tang et al.¹⁰²⁻¹⁰⁴ applied β -cyclodextrin (β -CD), a commonly used cyclic oligosaccharide drug carrier, to crosslink low molecular weight PEI (MW 600 Da) to form a high molecular weight cationic polymer that showed lower cytotoxicity and high transfection efficiency close to PEI 25 kDa. Another example is to modify the amine groups to lower the cyto-toxicity of PEI. It is known that cytotoxic T lymphocytes (CTL) and natural killer (NK) cells protect vertebrates by killing infected or transformed cells using granzyme B (GrB) to induce apoptosis, but GrB-induced apoptosis of target cells can cause inflammatory diseases and chronic transplant rejection. PEI has been used to deliver a plasmid encoding GrB inhibitor proteinase inhibitor-9 (PI-9) to prevent apoptosis of the target cells. To reduce the cyto-toxicity, PEI is modified by selectively blocking a portion of the primary amine groups with a mannose functionalized cyclic carbonate by simple nucleophilic addition chemistry. PEI with 7 or 20 of 67 primary amine groups substituted by the carbohydrate exhibits a similar gene binding ability as unmodified PEI resulting in

decreased cytotoxicity of PEI/DNA complexes¹⁰⁵.

The stability of gene and gene carriers in the physiological environment is crucial to gene delivery. Genes must survive degradation in the extracellular surroundings and be successfully transported into the targeted cell to perform the designed biological functions. Small interfering RNA (siRNA), sometimes known as short interfering RNA, has provided insights into the therapeutic mechanism of a variety of intractable diseases since it can induce potent sequence-specific gene silencing, termed RNA interference (RNAi)¹⁰⁶⁻¹⁰⁹. However, siRNA is very susceptible to degradation by serum nucleases and rapid elimination *via* the kidneys. These inherent drawbacks of siRNA compromise the *in vivo* gene silencing activity substantially and therefore, the use of carrier systems is necessary to achieve successful delivery to the cytoplasm of the target cell. Generally, the tolerability under physiological conditions and enhanced cellular uptake must be considered in the design of nano-carriers in gene delivery^{110, 111}. Gouda et al.¹¹² introduced silica nanogelling to modify poly(ethylene glycol) (PEG)-block-polycation/siRNA complexes (PEGylated polyplexes) to enhance the stability and functionality. Silica nanogelling was achieved by polycondensation of soluble silicates onto the surface of PEGylated polyplexes comprising a disulfide cross-linked core. Silica nanogelling substantially improved the polyplex stability against counter polyanion-induced dissociation under non-reductive conditions without compromising the reductive environment-responsive siRNA release triggered by disulfide cleavage. In addition,

silica nanogelling significantly enhanced the sequence-specific gene silencing activity of the polyplexes in HeLa cells without the associated cytotoxicity, probably due to lower endosomal entrapment (or lysosomal degradation) of delivered siRNA.

Besides reduced cytotoxicity and enhanced stability, surface functionalization is of importance to the design of polymeric nano-carriers in gene delivery. Dendrigraft poly-L-lysines (DGL), one of the non-viral vectors, have been used in gene delivery to tumors because of their ability to complex and condense DNA to form nanoparticles. Steric stabilization and tumor targeting can be obtained by grafting PEG and decorating activatable cell-penetrating peptide (dtACPP) on the nanoparticles, respectively. Fig. 11A shows the synthetic steps of PEG-DGL and dtACPPD. Here, dtACPP is conjugated to the surface of DGL *via* α -Maleimidyl- ω -N-hydroxysuccinimidyl polyethyleneglycol (MAL-PEG-NHS) to construct the gene nanocarrier, dtACPP-PEG-DGL (dtACPPD). The condensed nanoparticles, dtACPPD/DNA, are formed by electrostatic interactions between the cationic DGL and negatively charged plasmid DNA. Therefore, dtACPPD/DNA can efficiently protect and deliver intact DNA to the target tumor in *in vivo* gene transfection (Fig. 11B). As the cell-penetrating property of CPP is quenched in the circulation, these nanocarriers with steric stabilization will accumulate in the tumor sites *via* the enhanced permeability and retention (EPR) effect. After reaching the tumor, the pre-existing attraction effect is eliminated due to the lower pH in the tumor microenvironment. Furthermore, accompanying the cleavage of matrix

metalloproteinase 2 (MMP2) linker, dtACPP is activated to expose CPP to drive the nano-carriers into the tumor cells¹¹³.

3.2 Biomedical plasmonic gold nanostructures

Gold nanostructures (AuNSs) constitute a versatile platform in a broad range of biological and biomedical applications such as bio-sensing, imaging, and photo-thermal therapy due to surface plasmon resonance (SPR)^{114, 115}. SPR is an optical phenomenon caused by the interaction between an electromagnetic wave and the conduction electrons on a metal. The conduction electrons in a gold nanostructure are driven by the electric field to collectively oscillate at a resonant frequency under light irradiation and this resonant frequency is related to the lattice of the positive ions as well as composition, size, geometry, dielectric environment and particle-particle separation distance of the AuNSs^{116, 117}. Scattering and absorption are two important physical phenomena occurring at the same time in this process. In the biomedical fields, scattering and absorption in the near infrared region (NIR, 650-900 nm) are especially favored because light can penetrate deeply into tissues in this region due to low absorption from blood and water and scattering from tissues. Moreover, the heat generated from the photo-thermal effect can be exploited therapeutically due to hyperthermia. Tailoring the gold nanostructures morphology is a powerful route to obtain the desirable SPR in the NIR region because small changes in the aspect ratio or corner sharpness have a large impact on the SPR response. Gold nanospheres, gold nanorods, gold nanoshells, and gold nanocages

are the four main types of synthesized AuNSs. In addition, the gold nanostructures need to be conjugated with functional moieties such as antibodies, peptides, and folate to increase a number of the critical attributes because gold has a unreactive and relatively bio-inert nature¹¹⁸. Surface engineering of AuNPs broadens their applications effectively and in the following sections, we discuss with specific examples how these properties can be harnessed in biomedical applications including optical imaging, photo-thermal treatment, and drug delivery.

A good biological recognition system has the following important features: specificity, sensitivity, and reproducibility. Usually, specific molecular recognition is a fundamental prerequisite according to the affinity between complementary structures such as enzyme-substrate, antibody-antigen, and receptor-hormone. Concentration-dependent signals may be generated based on this behavior¹¹⁹. Gold nanostructures are promising to bio-sensing and bio-imaging due to their unique SPR effect as described above. Surface modification including that of the composition and morphology has been developed to improve the performance to satisfy different requirements. Wang et al.¹²⁰ modified gold nanorods (GNRs) by poly (allylamine hydrochloride) and conjugated them with Rose Bengal (RB) molecules to produce RB-GNRs for optical detection of cancer cells (Fig. 12). The modified gold nanorods exhibit good stability in an aqueous solution, low cytotoxicity, strong optical absorption in the near infrared region, and in particular, high specificity to oral cancer cells. RB-GNRs are used as the sensing probe for label-free sensing assay and to

monitor the aggregation-induced red-shift in the NIR absorption wavelength. In the specific and quantitative analysis of the oral cancer cell lysate, a low detection limit of 2,000 cells/mL is obtained. Recently, Dondapati et al.¹²¹ prepared a new type of gold nanostars to achieve high sensitivity in single nanoparticle label-free bio-sensing. These nanostars present multiple plasmon resonances of which the lower energy ones, corresponding to the nanostar tips and core-tip interactions, are the most sensitive to environmental changes. Streptavidin molecules are detected upon binding to individual, biotin-modified gold nanostars by spectral shifts in the plasmon resonances. Concentrations as small as 0.1 nM can be detected because it produces a shift of the tip-related plasmon resonance of about 2.3 nm (5.3 meV).

It is always desirable to accomplish molecular imaging for cancer cell diagnostics and selective photo-thermal cancer therapy simultaneously with high efficiency. A conventional strategy is to use agents that are active in the near infrared region (NIR) of the radiation spectrum. Gold nanostructures have good tunability in SPR absorption and good efficacy in converting light energy to heat in the NIR region¹²². Hence, gold nanostructures such as gold nanorods are one of the candidates in photo-thermal therapy and proper surface modification can further improve and broaden their applications. Huang et al.¹²³ conjugated gold nanorods to anti-epidermal growth factor receptor (anti-EGFR) monoclonal antibodies. Owing to the over-expressed EGFR on the cytoplasmic membrane of the malignant cells, the anti-EGFR antibody-conjugated nanorods bind specifically to the surface of the

malignant type cells with a higher affinity. The malignant cells are clearly visualized and diagnosed from the nonmalignant cells. After exposure to a continuous red laser at 800 nm, the malignant cells require about half the laser energy to be photo-thermally destroyed than the nonmalignant cells. Choi et al.¹²⁴ have developed a very effective hyperthermia system for successful photothermal cancer therapy. Gold nanorods that can absorb NIR light are loaded to the functional nanocarriers that provide stable storage of gold nanorods and selective delivery to a target tumor. These functional nanocarriers (chitosan-conjugated, Pluronic-based nanocarriers) are prepared by chemically cross-linking Pluronic F 68 with chitosan conjugation. When the gold nanorods are delivered by means of these nanocarriers, enhanced *in vitro* cellular uptake and photo-thermal effects are observed and intravenous injection of this system followed by NIR laser irradiation to the tumor can result in very efficient thermolysis *in vivo*.

Drug/gene delivery is an important application of gold nanostructures and two recent examples about Au nanocarriers in disease treatment are discussed here. Treatment of Alzheimer's disease and other brain-related disorder is limited because of the presence of the blood-brain barrier that highly regulates the crossing of drugs. Gold nanoparticles conjugated to the peptide CLPFFD can destroy the toxic aggregates of β -amyloid similar to the ones found in the brain of patients with Alzheimer's disease, but nanoparticles are very difficult to cross the blood-brain barrier. The peptide sequence THRPPMWSPVWP is introduced into the gold

nanoparticle-CLPFFD conjugate. This peptide sequence interacts with the transferrin receptor present in the microvascular endothelial cells of the blood-brain barrier to increase the permeability of the conjugate in the brain¹²⁵. Human immunodeficiency virus-1 (HIV-1) is one of the most catastrophic pandemics to mankind and Au nanorods (Au NRs) have been suggested as the possible vehicles for gene delivery in HIV treatment. Two cationic molecules, poly(diallyldimethylammonium chloride) (PDDAC) and polyethyleneimine (PEI), have been selected to modify the surface of Au NRs. These PDDAC or PEI modified Au NRs can significantly promote cellular and humoral immunity as well as T cell proliferation through activating antigen-presenting cells compared to naked HIV-1 Env plasmid DNA treatment *in vivo*¹²⁶.

Gold nanostructures have a bright future in the biomedical fields and chemical surface modification is a dominant approach to improve and extend their functions. However, the surface conjugated with other chemical species may introduce some potential side effects. Therefore, it is necessary to better understand the biological, physical, and chemical interactions between the modified gold nanostructures and living organs and associated mechanism to facilitate efficient design of gold nanostructure-based agents.

3.3 Biomedical super-paramagnetic ion oxide nanoparticles

Super-paramagnetism is an interesting phenomenon that occurs in magnetic

materials. When the size is reduced below that of a single magnetic domain, super-paramagnetic materials retain no remnant magnetization after removing the external magnetic field^{127, 128}. Super-paramagnetic iron oxide nanoparticles (SPIONs), one of the important super-paramagnetic materials, have attracted much attention in biotechnology and been used in various biomedical applications such as magnetic resonance imaging (MRI), localized hyperthermia, and drug delivery¹²⁹⁻¹³². Usually, the colloidal stability in water at neutral pH and physiological salinity is very critical for SPIONs and the particles must be small enough to avoid precipitation induced by gravitation. In addition, the charge and surface chemistry are important because they can give rise to both steric and coulombic repulsion^{133, 134}. Surface modification is commonly performed on SPIONs to improve the properties. For example, a surface coating not only renders the magnetic particles non-toxic and biocompatible, but also permits target delivery to a specific region. Both inorganic and polymeric materials have been used to improve the biocompatibility and dispersibility in an aqueous medium. When SPIONs have the proper surface architecture and are conjugated with targeting ligands/proteins, they are suitable for applications such as bio-imaging and drug delivery¹³⁵.

Internalization of SPIONs into specific cells is one of the critical steps in the delivery process. Zhang et al.¹³⁶ modified the surface with poly(ethylene glycol) (PEG) and folic acid to improve intracellular uptake and the ability to target specific cells of super-paramagnetic magnetite nanoparticles. After modification, they

investigated nanoparticle internalization into mouse macrophage (RAW 264.7) and human breast cancer (BT20) cells. The uptake amount of PEG-modified nanoparticles into macrophage cells was much smaller than that of the unmodified nanoparticles, whereas folic acid modification did not alter the uptake. However, both PEG and folic acid modification facilitated nanoparticle internalization into breast cancer cells. It means that PEG and folic acid modification of magnetic nanoparticles can resist protein adsorption thereby avoiding particle recognition by macrophage cells and facilitating nanoparticle uptake to specific cancer cells in cancer therapy and diagnosis.

A prevailing trend is to combine discrete functional components into a single nanostructure. Each component can possess specific advantages to complement each other in an all-in-one system. Magnetic iron oxide nanoparticles are good contrasting agents in T2-weighted magnetic resonance imaging (MRI). Although MRI offers high spatial and temporal resolution and excellent tissue penetration depth, it is not as sensitive as optical imaging or positron emission tomography and difficult to visualize in microscopic tissue examination^{137, 138}. Therefore, it will be more attractive if MRI is combined with other modalities such as optical imaging. Yan et al.¹³⁹ developed a stable and cyto-compatible and multi-functional nanoparticle probe in liver and spleen imaging with magnetic and fluorescent capabilities. They synthesized Fe₃O₄-encapsulated polymeric micelles composed of cores containing magnetic nanoparticles and polyethylene glycol (PEG) shells by self-assembly of

amphiphilic poly(-HFMA-co-VBK)-g-PEG copolymers and oleic acid stabilized Fe_3O_4 nanoparticles, where HFMA denotes 2,2,3,4,4,4-Hexafluorobutyl methacrylate and VBK denotes 9-(4-vinylbenzyl)-9H-carbazole. Fig. 13 shows the schematic illustrating the preparation process and TEM images of the polymeric micelles with magnetic nanoparticles. The Fe_3O_4 magnetic nanoparticles in the core produce T2-weighted MRI functionalities and the small fluorescent monomer carbazole in the polymer shell introduces good fluorescent properties. Obviously, the core-shell structures and related fabrication methods are new features evolving from recent advance in surface modification research on the micro- and nano- scale. In order to achieve multimodal imaging and other functions, other nanostructures including quantum dots have been combined with SPIONs. For example, Ye et al.¹⁴⁰ developed a core-shell micro-nano system consisting of polylactic-co-glycolic acid (PLGA) nanoparticles encapsulating super-paramagnetic iron oxide nanoparticles (SPIONs) for MRI and cadmium-free manganese-doped zinc sulfide (Mn:ZnS) quantum dots (QDs) in fluorescence imaging. The core-shell structure allows them to encapsulate and carry poorly water-soluble drugs and to release these drugs at a sustained rate in the optimal drug concentration range. Yang et al.¹⁴¹ combined two different functional nanomaterials, gold (Au) and iron oxide (IONP), into one structure to develop a kind of Affibody based trimodality nanoprobe in order to image epidermal growth factor receptor (EGFR) positive tumors. The IONP component served as a T2 reporter in MRI and gold component served as both the optical and PET reporters. Both targeting molecules (anti-EGFR Affibody protein) and PET

imaging reporters (radiometal ^{64}Cu chelators) could be anchored on the nanoprobe to realize surface-specific modification in a highly efficient and reliable manner. In short, with the advent of nanotechnology and use of novel nanomaterials in biomedical engineering and biotechnology, it is feasible to combine SPIONs with other nanostructures to construct all-in-one systems suitable for multi-modality imaging as well as therapy.

3.4 Graphene: a rising star in biomedical engineering and biotechnology

Graphene has attracted tremendous attention since its inception due to its unique electronic, thermal, mechanical, optical properties¹⁴²⁻¹⁴⁵. In addition to many other applications, graphene and related materials including graphene oxide (GO) are potential sensors in living systems and useful to drug and gene delivery, photo-thermal therapy, as well as tissue engineering^{146, 147}. As the materials are in living systems, their biocompatibility and toxicity have to be evaluated carefully because pristine graphene and graphene oxide (GO) can exhibit toxic effects to cells and animals¹⁴⁸⁻¹⁵⁰. Fortunately, surface modification can provide a convenient way to overcome these disadvantages in the bio-environment. For instance, functionalized nano-GO coated with biocompatible polymers such as polyethylene glycol or dextran appears to be not toxic^{151, 152}. Importantly, surface modification can functionalize graphene and its derivatives. By fabricating another type of nanostructure on the surface, multi-functions can be achieved. For instance, functional nanostructures such as gold nanorods, iron oxide nanoparticles, and

quantum dots can be combined with graphene and its derivatives in bioimaging, cancer diagnosis, drug delivery, and photo-thermal therapy.

Hu et al.¹⁵³ coupled core-shell CdSe/ZnS quantum dots (QDs) with graphene oxide (GO) to obtain QD-tagged reduced graphene oxide (QD-rGO) suitable for fluorescent cell imaging and phototherapy because QDs exhibit brighter fluorescence and narrower photoluminescence spectra. In their studies, the QDs toxicity was mitigated by a surfactant coating, and fluorescence quenching was reduced by maintaining a precisely controlled spacer between the QDs and the rGO. As the QD-rGO absorbed near-infrared (NIR) irradiation, cell killing was accomplished in photo-thermal therapy. Zedan et al.¹⁵⁴ attached gold nanoparticles onto GO to obtain plasmonic GO-Au nanocomposites. Photo-thermal energy conversion was enhanced and the improved photo-thermal effects could be tuned by controlling the shape and size of the gold nanostructures in order to increase the heating efficiency of the laser-induced size reduction of gold nanostructures. Ma et al.¹⁵⁵ introduced magnetic iron oxide nanoparticles (IONPs) onto the surface of graphene oxide (GO) to form a GO-IONP nanocomposite for multimodal imaging. To acquire a high stability in physiological solutions, it was functionalized by a biocompatible polyethylene glycol (PEG) polymer. After doxorubicin (DOX), a chemotherapy drug, was loaded onto the nanocomposite, magnetic targeted drug delivery was accomplished. In addition, it can be utilized in localized photo-thermal ablation of cancer cells guided by a magnetic field. Shi et al.¹⁵⁶ decorated graphene oxide (GO) with both iron oxide

nanoparticles (IONPs) and gold to form a multi-functional magnetic & plasmonic GO-IONP-Au nanocomposite which exhibited strong super-paramagnetism and enhanced optical absorbance in the near-infrared (NIR) region. Polyethylene glycol (PEG) was used to coat the nanocomposite to improve the stability in the physiological environment and reduce the toxicity. Remarkably enhanced photothermal cancer ablation effects were realized and magnetic resonance (MR) and X-ray dual-modal imaging was also achieved using the IONP and Au in the nanocomposite.

Graphene-based materials are also used in surface functionalization of other nanostructures. Jin et al.¹⁵⁷ introduced gold nanoparticles (Au NPs) into poly (lactic acid) (PLA) microcapsules to obtain theranostic microcapsules by a double-micro-emulsion method. They applied the electrostatic layer-by-layer self-assembly technique to deposit graphene oxide (GO) onto the microcapsule surface. Fig. 14A shows the schematic of the fabrication process and Fig. 14B depicts the morphology of the microcapsules. The PLA microcapsules not only enhance ultrasound (US) imaging but also load GO and Au NPs. The Au NPs serve as a contrast agent to enhance computed tomography (CT) imaging and GO acts as a strong NIR-light absorbing agent because it converts absorbed light into heat efficiently and possesses superior optical absorption in the near-infrared (NIR) region. The near infrared (NIR) laser light ablates the tumor completely within 9 days in the presence of the microcapsules and the tumor growth inhibition is 83.8%.

In brief, graphene is a rising star in biotechnology and opens many opportunities with respect to multimodal imaging and cancer therapy. However, most of the applications are still in the infancy stage and much effort must be made to realize clinical success, but nonetheless, surface functionalization is expected to play a major role.

4. Conclusion

Biomaterials in living systems are multifunctional, dynamic, and different from many types of other functional materials and the surface of biomaterials provides the platform for biological and chemical interactions. As most biomaterials do not possess all of the desirable properties, surface modification is often adopted in materials engineering and design. By employing various physical and chemical means, the surface composition and structure can be altered to facilitate seamless adaptation to the physiological surroundings and simultaneously perform the required functions. This paper reviews recent progress in surface modification and functionalization of biomaterials with emphasis on tissue engineering, drug and gene delivery, as well as disease diagnosis. With regard to metallic and polymeric biomaterials, surface modification serves to improve the biocompatibility and antimicrobial properties. In addition, the rate of natural degradation on Mg alloys used in orthopedic applications can be controlled by the proper modification protocols. For micro- and nano-systems made of organic or inorganic materials, surface

modification can improve the stability in the physiological environment, reduce the toxicity, and provide new functions for drug/gene delivery, disease diagnosis, and therapy. Since most biomaterials are still far from perfect, continuous refinement of the materials properties and design of new biomedical components require more knowledge and better understanding of the principles and mechanisms. The emergence of nanotechnology enables more intricate control of biological functions and the interface between cells and biomaterials. In order to produce biomaterials that are more compatible, controllable, and smarter, surface modification is expected to continue to play a major role and attract the interest of researchers and technologists.

Acknowledgments

This work was financially supported by Hong Kong Research Grants Council (RGC) General Research Funds (GRF) No. CityU 112212, City University of Hong Kong Applied Research Grant (ARG) No. 9667085, and City University of Hong Kong Strategic Research Grant (SRG) No. 7004188. The authors would like to thank Dr. Ying Zhao (Shenzhen Institutes of Advanced Technology, Chinese Academy of Sciences, China) for helpful discussion.

Biographies & photographs

Guosong Wu received his PhD in materials processing engineering from Shanghai Jiao Tong University (China) in 2007. After graduation, he joined Chinese Academy of Sciences (China) as a postdoctoral fellow in 2007 and was promoted to associate professor in 2010. He joined Prof. Paul K Chu research group at City University of Hong Kong as senior research associate in 2010 and is presently research fellow. His research interests include surface engineering, thin solid films, corrosion science, and biomaterials.

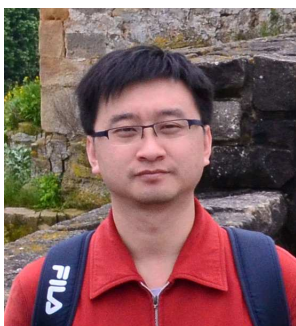


Penghui Li received his BS and MS in polymer science and engineering from Hubei University (China) in 2008 and 2011, respectively. Afterwards, he joined the

research group of Professor Paul K Chu at City University of Hong Kong and received his PhD under Prof. Chu's guidance in 2014. He is currently affiliated with the Shenzhen Institutes of Advanced Technology. His research interests include functional polymer microspheres, polymer films/coatings, and surface modification for biomedical applications.



Hongqing Feng received her PhD in biomedical engineering from Peking University (China) in 2011. After graduation, she worked as a postdoctoral fellow in Peking University from 2012 to 2014 and is presently a senior research associate in Professor Paul K Chu's group at City University of Hong Kong (China). Her research interests include biomedical plasma applications and biomaterials.



Xuming Zhang received his BS from Wuhan University of Technology (China) and MS in materials science from Wuhan University of Science and Technology (China) in 2004 and 2010, respectively. Now, He is currently a doctoral student at City University of Hong Kong under the supervision of Professor Paul K Chu. His research interests include biomaterials, electrochemical sensors, and electrochemical energy storage devices.



Paul K. Chu received his BS in mathematics from The Ohio State University and MS and PhD in Chemistry from Cornell University. His research interests are quite diverse encompassing plasma surface engineering, materials science and engineering, as well as surface science. He is Chair Professor of Materials Engineering in the Department of Physics and Materials Science at City University of Hong Kong. He is a Fellow of the APS, AVS, IEEE and MRS. He is also Fellow of the Hong Kong Academy of Engineering Sciences.

References

1. N. Huebsch and D. J. Mooney, *Nature*, 2009, 462, 426-432.
2. N. Peppas and R. Langer, *Science*, 1994, 263, 1715-1720.
3. Y. Liao, R. Pourzal, M. A. Wimmer, J. J. Jacobs, A. Fischer and L. D. Marks, *Science*, 2011, 334, 1687-1690.
4. S. Parveen, R. Misra and S. K. Sahoo, *Nanomed., Nanotech. Biol. Med.*, 2012, 8, 147-166.
5. A. E. Nel, L. Madler, D. Velegol, T. Xia, E. M. V. Hoek, P. Somasundaran, F. Klaessig, V. Castranova and M. Thompson, *Nat. Mater.*, 2009, 8, 543-557.
6. C. J. Kearney and D. J. Mooney, *Nat. Mater.*, 2013, 12, 1004-1017.
7. K. Wu, W. Song, L. Zhao, M. Liu, J. Yan, M. Ø. Andersen, J. Kjems, S. Gao and Y. Zhang, *ACS Appl. Mater. Interfaces*, 2013, 5, 2733-2744.
8. N. D. Evans and E. Gentleman, *J. Mater. Chem. B*, 2014, 2, 2345-2356.
9. S. Mitragotri and J. Lahann, *Nat. Mater.*, 2009, 8, 15-23.
10. P. K. Chu, *Thin Solid Films*, 2013, 528, 93-105.
11. L. Zhang, Y. Li and J. C. Yu, *J. Mater. Chem. B*, 2014, 2, 452-470.
12. X. Liu, P. K. Chu and C. Ding, *Mater. Sci. Eng., R*, 2004, 47, 49-121.
13. K. G. Neoh, X. Hu, D. Zheng and E. T. Kang, *Biomaterials*, 2012, 33, 2813-2822.
14. S. Wu, X. Liu, A. Yeung, K. W. K. Yeung, R. Y. T. Kao, G. Wu, T. Hu, Z. Xu and P. K. Chu, *ACS Appl. Mater. Interfaces*, 2011, 3, 2851-2860.
15. S. B. Goodman, Z. Yao, M. Keeney and F. Yang, *Biomaterials*, 2013, 34,

- 3174-3183.
16. P. K. Chu, J. Y. Chen, L. P. Wang and N. Huang, *Mater. Sci. Eng., R*, 2002, 36, 143-206.
 17. S. Wu, X. Liu, K. W. K. Yeung, C. Liu and X. Yang, *Mater. Sci. Eng., R*, 2014, 80, 1-36.
 18. S. Wu, C. Y. Chung, X. Liu, P. K. Chu, J. P. Y. Ho, C. L. Chu, Y. L. Chan, K. W. K. Yeung, W. W. Lu, K. M. C. Cheung and K. D. K. Luk, *Acta Mater.*, 2007, 55, 3437-3451.
 19. S. Wu, X. Liu, K. W. K. Yeung, T. Hu, Z. Xu, J. C. Y. Chung and P. K. Chu, *Acta Biomater.*, 2011, 7, 1387-1397.
 20. K. W. K. Yeung, R. W. Y. Poon, P. K. Chu, C. Y. Chung, X. Y. Liu, W. W. Lu, D. Chan, S. C. W. Chan, K. D. K. Luk and K. M. C. Cheung, *J. Biomed. Mater. Res., A*, 2007, 82A, 403-414.
 21. S. Wu, X. Liu, Y. L. Chan, J. P. Y. Ho, C. Y. Chung, P. K. Chu, C. L. Chu, K. W. K. Yeung, W. W. Lu, K. M. C. Cheung and K. D. K. Luk, *J. Biomed. Mater. Res., A*, 2007, 81A, 948-955.
 22. Y. Zhao, S. M. Wong, H. M. Wong, S. Wu, T. Hu, K. W. K. Yeung and P. K. Chu, *ACS Appl. Mater. Interfaces*, 2013, 5, 1510-1516.
 23. H. Cao, X. Liu, F. Meng and P. K. Chu, *Biomaterials*, 2011, 32, 693-705.
 24. J. Gómez-Morales, M. Iafisco, J. M. Delgado-López, S. Sarda and C. Drouet, *Prog. Cryst. Growth Charact. Mater.*, 2013, 59, 1-46.
 25. A. R. Boyd, H. Duffy, R. McCann, M. L. Cairns and B. J. Meenan, *Nucl.*

- Instrum. Methods Phys. Res., Sect. B*, 2007, 258, 421-428.
26. H. Li, K. A. Khor and P. Cheang, *Biomaterials*, 2003, 24, 949-957.
 27. H. Li, K. A. Khor and P. Cheang, *Biomaterials*, 2004, 25, 3463-3471.
 28. Y. W. Gu, K. A. Khor, D. Pan and P. Cheang, *Biomaterials*, 2004, 25, 3177-3185.
 29. H. S. Alghamdi, R. Bosco, J. J. J. P. van den Beucken, X. F. Walboomers and J. A. Jansen, *Biomaterials*, 2013, 34, 3747-3757.
 30. R. Guillot, F. Gilde, P. Becquart, F. Sailhan, A. Lapeyrere, D. Logeart-Avramoglou and C. Picart, *Biomaterials*, 2013, 34, 5737-5746.
 31. C. Yue, R. Kuijjer, H. J. Kaper, H. C. van der Mei and H. J. Busscher, *Biomaterials*, 2014, 35, 2580-2587.
 32. X. Liu, P. K. Chu and C. Ding, *Mater. Sci. Eng., R*, 2010, 70, 275-302.
 33. L. Zhao, S. Mei, P. K. Chu, Y. Zhang and Z. Wu, *Biomaterials*, 2010, 31, 5072-5082.
 34. N. Tsukimura, M. Yamada, F. Iwasa, H. Minamikawa, W. Att, T. Ueno, L. Saruwatari, H. Aita, W.-A. Chiou and T. Ogawa, *Biomaterials*, 2011, 32, 4358-4368.
 35. J. Li, X. Liu, Y. Qiao, H. Zhu and C. Ding, *Colloids Surf., B*, 2014, 113, 134-145.
 36. Y.-H. Lee, G. Bhattarai, I.-S. Park, G.-R. Kim, G.-E. Kim, M.-H. Lee and H.-K. Yi, *Biomaterials*, 2013, 34, 10199-10208.
 37. A. Gao, R. Hang, X. Huang, L. Zhao, X. Zhang, L. Wang, B. Tang, S. Ma and

- P. K. Chu, *Biomaterials*, 2014, 35, 4223-4235.
38. S. Mei, H. Wang, W. Wang, L. Tong, H. Pan, C. Ruan, Q. Ma, M. Liu, H. Yang, L. Zhang, Y. Cheng, Y. Zhang, L. Zhao and P. K. Chu, *Biomaterials*, 2014, 35, 4255-4265.
39. K. Gulati, S. Ramakrishnan, M. S. Aw, G. J. Atkins, D. M. Findlay and D. Lopic, *Acta Biomater.*, 2012, 8, 449-456.
40. O. Z. Andersen, V. Offermanns, M. Sillassen, K. P. Almqvist, I. H. Andersen, S. Sørensen, C. S. Jeppesen, D. C. E. Kraft, J. Böttiger, M. Rasse, F. Kloss and M. Foss, *Biomaterials*, 2013, 34, 5883-5890.
41. Y. Xin, J. Jiang, K. Huo, T. Hu and P. K. Chu, *ACS Nano*, 2009, 3, 3228-3234.
42. L. Zhao, H. Wang, K. Huo, X. Zhang, W. Wang, Y. Zhang, Z. Wu and P. K. Chu, *Biomaterials*, 2013, 34, 19-29.
43. R. Zeng, W. Dietzel, F. Witte, N. Hort and C. Blawert, *Adv. Eng. Mater.*, 2008, 10, B3-B14.
44. G. Song, *Corros. Sci.*, 2007, 49, 1696-1701.
45. A. C. Hänzi, P. Gunde, M. Schinhammer and P. J. Uggowitzer, *Acta Biomater.*, 2009, 5, 162-171.
46. B. Zberg, P. J. Uggowitzer and J. F. Löffler, *Nat. Mater.*, 2009, 8, 887-891.
47. E. Zhang, L. Xu and K. Yang, *Scripta Mater.*, 2005, 53, 523-527.
48. Y. F. Zheng, X. N. Gu and F. Witte, *Mater. Sci. Eng., R*, 2014, 77, 1-34.
49. M. P. Staiger, A. M. Pietak, J. Huadmai and G. Dias, *Biomaterials*, 2006, 27, 1728-1734.

50. F. Witte, V. Kaese, H. Haferkamp, E. Switzer, A. Meyer-Lindenberg, C. J. Wirth and H. Windhagen, *Biomaterials*, 2005, 26, 3557-3563.
51. T. Kraus, S. F. Fischerauer, A. C. Hänzli, P. J. Uggowitzer, J. F. Löffler and A. M. Weinberg, *Acta Biomater.*, 2012, 8, 1230-1238.
52. G. Wu, Y. Zhao, X. Zhang, J. M. Ibrahim and P. K. Chu, *Corros. Sci.*, 2013, 68, 279-285.
53. Y. Zhao, G. Wu, J. Jiang, H. M. Wong, K. W. K. Yeung and P. K. Chu, *Corros. Sci.*, 2012, 59, 360-365.
54. L. Mao, L. Shen, J. Niu, J. Zhang, W. Ding, Y. Wu, R. Fan and G. Yuan, *Nanoscale*, 2013, 5, 9517-9522.
55. Y. Zong, G. Yuan, X. Zhang, L. Mao, J. Niu and W. Ding, *Mater. Sci. Eng., B*, 2012, 177, 395-401.
56. L. Mao, G. Yuan, J. Niu, Y. Zong and W. Ding, *Mater. Sci. Eng., C*, 2013, 33, 242-250.
57. G. Wu, J. M. Ibrahim and P. K. Chu, *Surf. Coat. Technol.*, 2013, 233, 2-12.
58. G. Song, B. Johannesson, S. Hapugoda and D. StJohn, *Corros. Sci.*, 2004, 46, 955-977.
59. J. Niu, G. Yuan, Y. Liao, L. Mao, J. Zhang, Y. Wang, F. Huang, Y. Jiang, Y. He and W. Ding, *Mater. Sci. Eng., C*, 2013, 33, 4833-4841.
60. L. Xu, F. Pan, G. Yu, L. Yang, E. Zhang and K. Yang, *Biomaterials*, 2009, 30, 1512-1523.
61. Y. W. Song, D. Y. Shan and E. H. Han, *Mater. Lett.*, 2008, 62, 3276-3279.

62. H. Wang, S. Guan, Y. Wang, H. Liu, H. Wang, L. Wang, C. Ren, S. Zhu and K. Chen, *Colloids Surf., B*, 2011, 88, 254-259.
63. T. S. N. Sankara Narayanan, I. S. Park and M. H. Lee, *Prog. Mater. Sci.*, 2014, 60, 1-71.
64. X. N. Gu, N. Li, W. R. Zhou, Y. F. Zheng, X. Zhao, Q. Z. Cai and L. Ruan, *Acta Biomater.*, 2011, 7, 1880-1889.
65. H. S. Ryu and S.-H. Hong, *J. Electrochem. Soc.*, 2010, 157, C131-C136.
66. S. F. Fischerauer, T. Kraus, X. Wu, S. Tangl, E. Sorantin, A. C. Hänni, J. F. Löffler, P. J. Uggowitzer and A. M. Weinberg, *Acta Biomater.*, 2013, 9, 5411-5420.
67. R. Xu, G. Wu, X. Yang, T. Hu, Q. Lu and P. K. Chu, *Mater. Lett.*, 2011, 65, 2171-2173.
68. G. Wu, K. Feng, A. Shanaghi, Y. Zhao, R. Xu, G. Yuan and P. K. Chu, *Surf. Coat. Technol.*, 2012, 206, 3186-3195.
69. Y. Zhao, G. Wu, Q. Lu, J. Wu, R. Xu, K. W. K. Yeung and P. K. Chu, *Thin Solid Films*, 2013, 529, 407-411.
70. Y. Zhao, G. Wu, H. Pan, K. W. K. Yeung and P. K. Chu, *Mater. Chem. Phys.*, 2012, 132, 187-191.
71. M. I. Jamesh, G. Wu, Y. Zhao, D. R. McKenzie, M. M. M. Bilek and P. K. Chu, *Corros. Sci.*, 2014, 82, 7-26.
72. Y. Zhao, M. I. Jamesh, W. K. Li, G. Wu, C. Wang, Y. Zheng, K. W. K. Yeung and P. K. Chu, *Acta Biomater.*, 2014, 10, 544-556.

73. G. Wu, X. Zhang, Y. Zhao, J. M. Ibrahim, G. Yuan and P. K. Chu, *Corros. Sci.*, 2014, 78, 121-129.
74. G. Wu, L. Sun, W. Dai, L. Song and A. Wang, *Surf. Coat. Technol.*, 2010, 204, 2193-2196.
75. G. Wu, W. Dai, H. Zheng and A. Wang, *Surf. Coat. Technol.*, 2010, 205, 2067-2073.
76. G. Wu, K. Ding, X. Zeng, X. Wang and S. Yao, *Scripta Mater.*, 2009, 61, 269-272.
77. R. Xu, X. Yang, P. Li, K. W. Suen, G. Wu and P. K. Chu, *Corros. Sci.*, 2014, 82, 173-179.
78. Y.-F. Huang, J.-Z. Xu, J.-S. Li, B.-X. He, L. Xu and Z.-M. Li, *Biomaterials*, 2014, 35, 6687-6697.
79. M. Kyomoto, T. Moro, K. Saiga, M. Hashimoto, H. Ito, H. Kawaguchi, Y. Takatori and K. Ishihara, *Biomaterials*, 2012, 33, 4451-4459.
80. T. Gumpenberger, J. Heitz, D. Bäuerle, H. Kahr, I. Graz, C. Romanin, V. Svorcik and F. Leisch, *Biomaterials*, 2003, 24, 5139-5144.
81. D. V. Bax, D. R. McKenzie, A. S. Weiss and M. M. M. Bilek, *Biomaterials*, 2010, 31, 2526-2534.
82. K. Cai, K. Yao, S. Lin, Z. Yang, X. Li, H. Xie, T. Qing and L. Gao, *Biomaterials*, 2002, 23, 1153-1160.
83. Y. L. Cui, A. D. Qi, W. G. Liu, X. H. Wang, H. Wang, D. M. Ma and K. D. Yao, *Biomaterials*, 2003, 24, 3859-3868.

84. T. Lu, X. Liu, S. Qian, H. Cao, Y. Qiao, Y. Mei, P. K. Chu and C. Ding, *Biomaterials*, 2014, 35, 5731-5740.
85. A. H. C. Poulsson, D. Eglin, S. Zeiter, K. Camenisch, C. Sprecher, Y. Agarwal, D. Nehrbass, J. Wilson and R. G. Richards, *Biomaterials*, 2014, 35, 3717-3728.
86. S. M. Kurtz and J. N. Devine, *Biomaterials*, 2007, 28, 4845-4869.
87. W. Zhang, Y. Luo, H. Wang, J. Jiang, S. Pu and P. K. Chu, *Acta Biomater.*, 2008, 4, 2028-2036.
88. H. Wang, J. Ji, W. Zhang, W. Wang, Y. Zhang, Z. Wu, Y. Zhang and P. K. Chu, *Acta Biomater.*, 2010, 6, 154-159.
89. H. Wang, D. T. K. Kwok, W. Wang, Z. Wu, L. Tong, Y. Zhang and P. K. Chu, *Biomaterials*, 2010, 31, 413-419.
90. C.-M. Han, E.-J. Lee, H.-E. Kim, Y.-H. Koh, K. N. Kim, Y. Ha and S.-U. Kuh, *Biomaterials*, 2010, 31, 3465-3470.
91. X.-T. Luo, C.-X. Li, F.-L. Shang, G.-J. Yang, Y.-Y. Wang and C.-J. Li, *Surf. Coat. Technol.*, 2014, 254, 11-20.
92. P. C. King, C. Busch, T. Kittel-Sherri, M. Jahedi and S. Gulizia, *Surf. Coat. Technol.*, 2014, 239, 191-199.
93. E. J. T. Pialago and C. W. Park, *Appl. Surf. Sci.*, 2014, 308, 63-74.
94. J. H. Lee, H. L. Jang, K. M. Lee, H.-R. Baek, K. Jin, K. S. Hong, J. H. Noh and H.-K. Lee, *Acta Biomater.*, 2013, 9, 6177-6187.
95. Y. Zhao, H. M. Wong, W. Wang, P. Li, Z. Xu, E. Y. W. Chong, C. H. Yan, K. W.

- K. Yeung and P. K. Chu, *Biomaterials*, 2013, 34, 9264-9277.
96. Z. Yue, X. Liu, P. J. Molino and G. G. Wallace, *Biomaterials*, 2011, 32, 4714-4724.
97. D. Putnam, *Nat. Mater.*, 2006, 5, 439-451.
98. H. Huang, H. Yu, G. Tang, Q. Wang and J. Li, *Biomaterials*, 2010, 31, 1830-1838.
99. W. T. Godbey, K. K. Wu and A. G. Mikos, *J. Controlled Release*, 1999, 60, 149-160.
100. W. T. Godbey, K. K. Wu and A. G. Mikos, *J. Biomed. Mater. Res.*, 1999, 45, 268-275.
101. D. Fischer, Y. Li, B. Ahlemeyer, J. Krieglstein and T. Kissel, *Biomaterials*, 2003, 24, 1121-1131.
102. D. Li, Y. Li, H. Xing, J. Guo, Y. Ping and G. Tang, *Adv. Funct. Mater.*, 2014, 24, 5482-5492.
103. G. P. Tang, H. Y. Guo, F. Alexis, X. Wang, S. Zeng, T. M. Lim, J. Ding, Y. Y. Yang and S. Wang, *J. Gene. Med.*, 2006, 8, 736-744.
104. Q. Hu, J. Wang, J. Shen, M. Liu, X. Jin, G. Tang and P. K. Chu, *Biomaterials*, 2012, 33, 1135-1145.
105. W. Cheng, C. Yang, J. L. Hedrick, D. F. Williams, Y. Y. Yang and P. G. Ashton-Rickardt, *Biomaterials*, 2013, 34, 3697-3705.
106. S. M. Elbashir, J. Harborth, W. Lendeckel, A. Yalcin, K. Weber and T. Tuschl, *Nature*, 2001, 411, 494-498.

107. A. Fire, S. Xu, M. K. Montgomery, S. A. Kostas, S. E. Driver and C. C. Mello, *Nature*, 1998, 391, 806-811.
108. M.-Y. Lee, S.-J. Park, K. Park, K. S. Kim, H. Lee and S. K. Hahn, *ACS Nano*, 2011, 5, 6138-6147.
109. Y. Nakamura, K. Kogure, S. Futaki and H. Harashima, *J. Controlled Release*, 2007, 119, 360-367.
110. K. Itaka, N. Kanayama, N. Nishiyama, W.-D. Jang, Y. Yamasaki, K. Nakamura, H. Kawaguchi and K. Kataoka, *J. Am. Chem. Soc.*, 2004, 126, 13612-13613.
111. N. Singh, A. Agrawal, A. K. L. Leung, P. A. Sharp and S. N. Bhatia, *J. Am. Chem. Soc.*, 2010, 132, 8241-8243.
112. N. Gouda, K. Miyata, R. J. Christie, T. Suma, A. Kishimura, S. Fukushima, T. Nomoto, X. Liu, N. Nishiyama and K. Kataoka, *Biomaterials*, 2013, 34, 562-570.
113. S. Huang, K. Shao, Y. Kuang, Y. Liu, J. Li, S. An, Y. Guo, H. Ma, X. He and C. Jiang, *Biomaterials*, 2013, 34, 5294-5302.
114. Y. Jin, *Adv. Mater.*, 2012, 24, 5153-5165.
115. J. Cao, T. Sun and K. T. V. Grattan, *Sens. Actuator B-Chem.*, 2014, 195, 332-351.
116. M. Hu, J. Chen, Z.-Y. Li, L. Au, G. V. Hartland, X. Li, M. Marquez and Y. Xia, *Chem. Soc. Rev.*, 2006, 35, 1084-1094.
117. E. Petryayeva and U. J. Krull, *Anal. Chim. Acta*, 2011, 706, 8-24.
118. C. M. Cobley, J. Chen, E. C. Cho, L. V. Wang and Y. Xia, *Chem. Soc. Rev.*,

- 2011, 40, 44-56.
119. S. Wu, Z. Weng, X. Liu, K. W. K. Yeung and P. K. Chu, *Adv. Funct. Mater.*, 2014, 24, 5464-5481.
120. J.-H. Wang, B. Wang, Q. Liu, Q. Li, H. Huang, L. Song, T.-Y. Sun, H. Wang, X.-F. Yu, C. Li and P. K. Chu, *Biomaterials*, 2013, 34, 4274-4283.
121. S. K. Dondapati, T. K. Sau, C. Hrelescu, T. A. Klar, F. D. Stefani and J. Feldmann, *ACS Nano*, 2010, 4, 6318-6322.
122. J. Wang, B. Dong, B. Chen, Z. Jiang and H. Song, *Dalton Trans.*, 2012, 41, 11134-11144.
123. X. Huang, I. H. El-Sayed, W. Qian and M. A. El-Sayed, *J. Am. Chem. Soc.*, 2006, 128, 2115-2120.
124. W. I. Choi, J.-Y. Kim, C. Kang, C. C. Byeon, Y. H. Kim and G. Tae, *ACS Nano*, 2011, 5, 1995-2003.
125. R. Prades, S. Guerrero, E. Araya, C. Molina, E. Salas, E. Zurita, J. Selva, G. Egea, C. López-Iglesias, M. Teixidó, M. J. Kogan and E. Giralt, *Biomaterials*, 2012, 33, 7194-7205.
126. L. Xu, Y. Liu, Z. Chen, W. Li, Y. Liu, L. Wang, Y. Liu, X. Wu, Y. Ji, Y. Zhao, L. Ma, Y. Shao and C. Chen, *Nano Lett.*, 2012, 12, 2003-2012.
127. J. E. Rosen, L. Chan, D.-B. Shieh and F. X. Gu, *Nanomed., Nanotech. Biol. Med.*, 2012, 8, 275-290.
128. A. S. Teja and P.-Y. Koh, *Prog. Cryst. Growth Charact. Mater.*, 2009, 55, 22-45.

129. Y. C. Park, J. B. Smith, T. Pham, R. D. Whitaker, C. A. Sucato, J. A. Hamilton, E. Bartolak-Suki and J. Y. Wong, *Colloids Surf., B*, 2014, 119, 106-114.
130. M. Darroudi, M. Hakimi, E. Goodarzi and R. Kazemi Oskuee, *Ceram. Int.*, 2014, 40, 14641-14645.
131. S. Klein, A. Sommer, L. V. R. Distel, W. Neuhuber and C. Kryschi, *Biochem. Biophys. Res. Commun.*, 2012, 425, 393-397.
132. N. Singh, G. J. S. Jenkins, B. C. Nelson, B. J. Marquis, T. G. G. Maffei, A. P. Brown, P. M. Williams, C. J. Wright and S. H. Doak, *Biomaterials*, 2012, 33, 163-170.
133. M. Mahmoudi, S. Sant, B. Wang, S. Laurent and T. Sen, *Adv. Drug Deliv. Rev.*, 2011, 63, 24-46.
134. P. Tartaj and C. J. Serna, *J. Am. Chem. Soc.*, 2003, 125, 15754-15755.
135. A. K. Gupta and M. Gupta, *Biomaterials*, 2005, 26, 3995-4021.
136. Y. Zhang, N. Kohler and M. Zhang, *Biomaterials*, 2002, 23, 1553-1561.
137. Y. Jin, C. Jia, S.-W. Huang, M. O'Donnell and X. Gao, *Nat. Commun.*, 2010, 1, 41.
138. R. Weissleder, *Nat. Rev. Cancer*, 2002, 2, 11-18.
139. K. Yan, H. Li, P. Li, H. Zhu, J. Shen, C. Yi, S. Wu, K. W. K. Yeung, Z. Xu, H. Xu and P. K. Chu, *Biomaterials*, 2014, 35, 344-355.
140. F. Ye, Å. Barrefelt, H. Asem, M. Abedi-Valugerdi, I. El-Serafi, M. Saghafian, K. Abu-Salah, S. Alrokayan, M. Muhammed and M. Hassan, *Biomaterials*, 2014, 35, 3885-3894.

141. M. Yang, K. Cheng, S. Qi, H. Liu, Y. Jiang, H. Jiang, J. Li, K. Chen, H. Zhang and Z. Cheng, *Biomaterials*, 2013, 34, 2796-2806.
142. A. K. Geim and K. S. Novoselov, *Nat. Mater.*, 2007, 6, 183-191.
143. A. K. Geim, *Science*, 2009, 324, 1530-1534.
144. F. Ma, Z. Guo, K. Xu and P. K. Chu, *Solid State Commun.*, 2012, 152, 1089-1093.
145. F. Ma, Y. J. Sun, D. Y. Ma, K. W. Xu and P. K. Chu, *Acta Mater.*, 2011, 59, 6783-6789.
146. J. Liu, L. Cui and D. Losic, *Acta Biomater.*, 2013, 9, 9243-9257.
147. Y. Wang, H. Chang, H. Wu and H. Liu, *J. Mater. Chem. B*, 2013, 1, 3521-3534.
148. K. Wang, J. Ruan, H. Song, J. Zhang, Y. Wo, S. Guo and D. Cui, *Nanoscale Res. Lett.*, 2011, 6, 8.
149. Y. Zhang, S. F. Ali, E. Dervishi, Y. Xu, Z. Li, D. Casciano and A. S. Biris, *ACS Nano*, 2010, 4, 3181-3186.
150. M. C. Duch, G. R. S. Budinger, Y. T. Liang, S. Soberanes, D. Urich, S. E. Chiarella, L. A. Campochiaro, A. Gonzalez, N. S. Chandel, M. C. Hersam and G. M. Mutlu, *Nano Lett.*, 2011, 11, 5201-5207.
151. K. Yang, J. Wan, S. Zhang, Y. Zhang, S.-T. Lee and Z. Liu, *ACS Nano*, 2010, 5, 516-522.
152. S. Zhang, K. Yang, L. Feng and Z. Liu, *Carbon*, 2011, 49, 4040-4049.
153. S.-H. Hu, Y.-W. Chen, W.-T. Hung, I. W. Chen and S.-Y. Chen, *Adv. Mater.*,

- 2012, 24, 1748-1754.
154. A. F. Zedan, S. Moussa, J. Turner, G. Atkinson and M. S. El-Shall, *ACS Nano*, 2012, 7, 627-636.
155. X. Ma, H. Tao, K. Yang, L. Feng, L. Cheng, X. Shi, Y. Li, L. Guo and Z. Liu, *Nano Res.*, 2012, 5, 199-212.
156. X. Shi, H. Gong, Y. Li, C. Wang, L. Cheng and Z. Liu, *Biomaterials*, 2013, 34, 4786-4793.
157. Y. Jin, J. Wang, H. Ke, S. Wang and Z. Dai, *Biomaterials*, 2013, 34, 4794-4802.

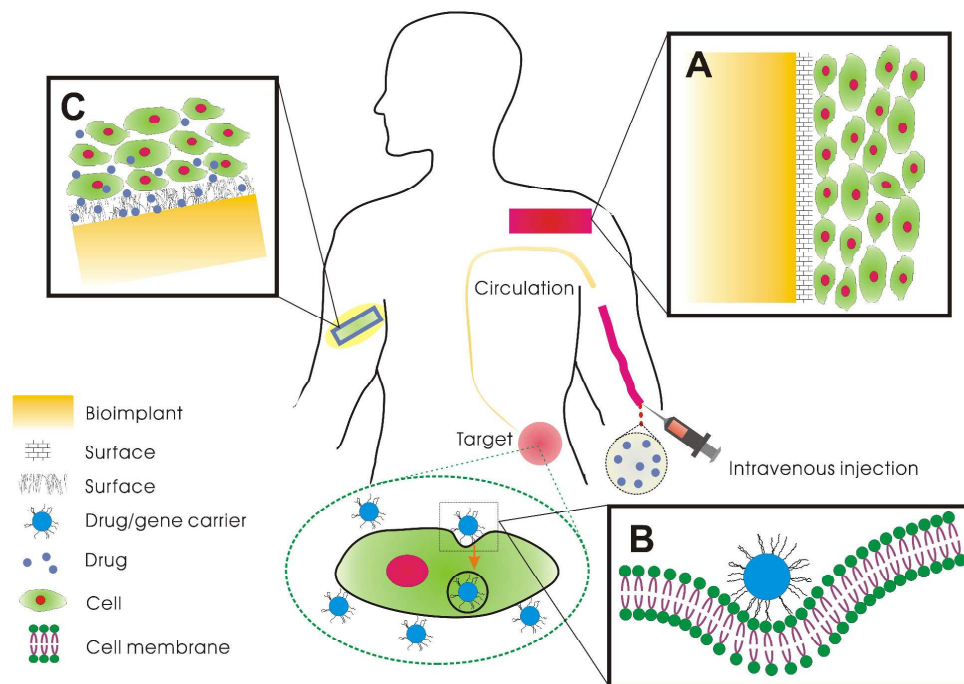


Fig. 1. Surface functions and roles of biomaterials.

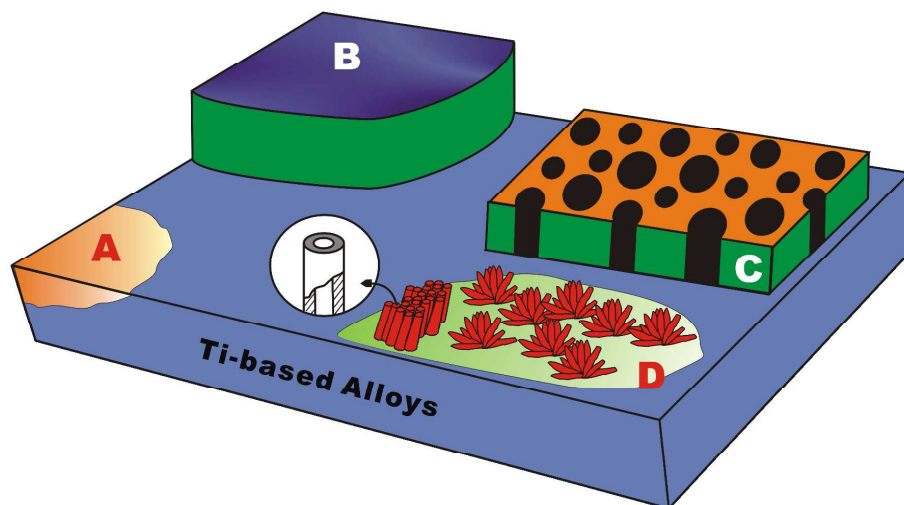


Fig. 2. Various types of modified surfaces on Ti-based alloys: (A) *In situ* reconstructed surfaces, (B) Dense coatings, (C) Porous coatings and (D) Nanostructures such as nano-flowers and nano-tubes.

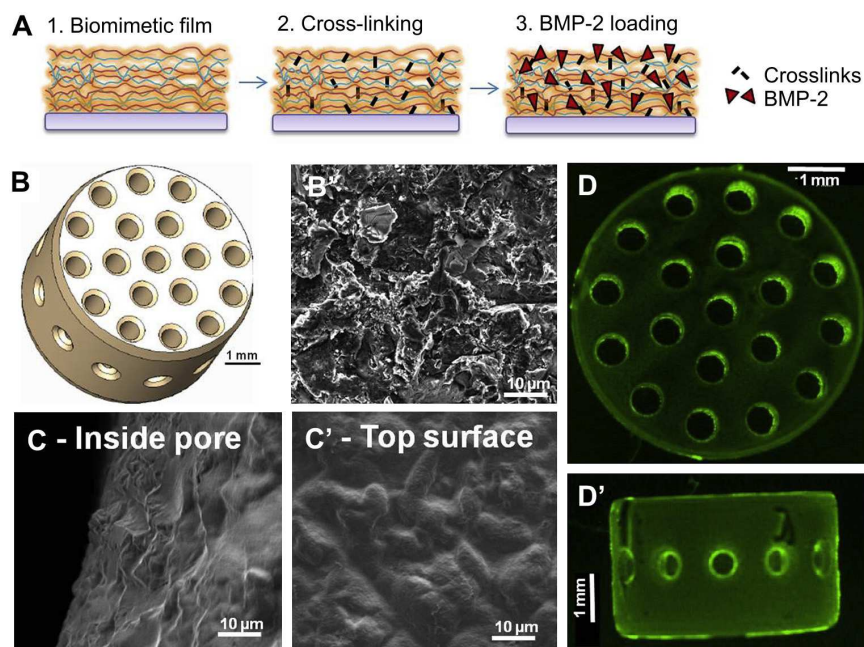


Fig. 3. Polyelectrolyte multilayered films on titanium substrate: (A) Three-step bioactive film preparation – (1) Film deposition by layer-by-layer assembly on the substrate, (2) Cross-linking, and (3) BMP-2 loading. (B) Schematic of porous TA6V scaffold with 500 mm pore size. (B') SEM micrograph of the uncoated TA6V surface on the implant surface. (C) SEM micrographs of (PLL/HA) 24 film-coated surface of the TA6V scaffold inside a pore channel or (C') on the outer surface. PEM-film deposited on the TA6V scaffold: (D) Top view and (D') Side view. Reprinted from ref. 30, copyright (2014), with permission from Elsevier.

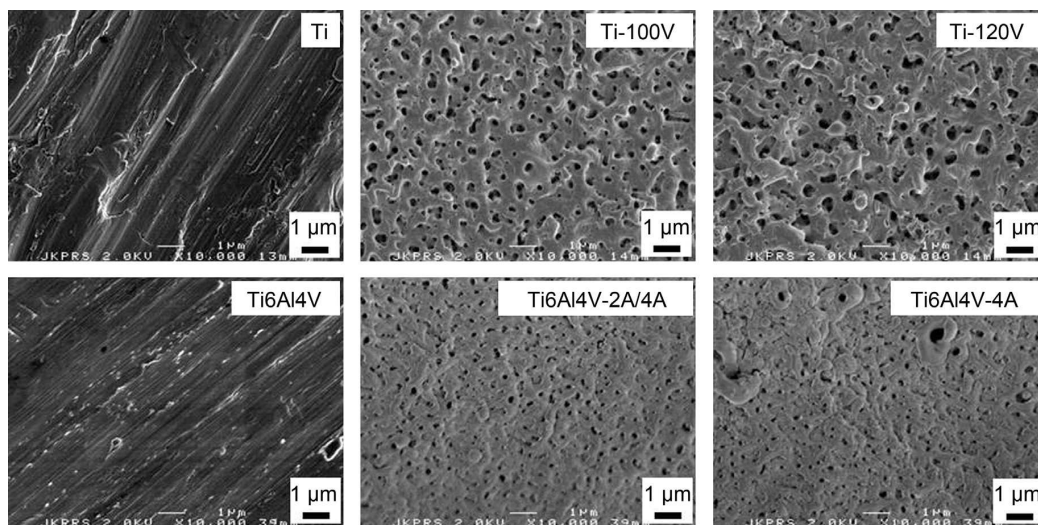


Fig. 4. Scanning electron micrographs of titanium (top row) and titanium alloy (bottom row) after anodic oxidation under different conditions. The porous structures are formed by anodization and pore size depends on the anodizing voltage and current density. Reprinted from ref. 31, copyright (2014), with permission from Elsevier.

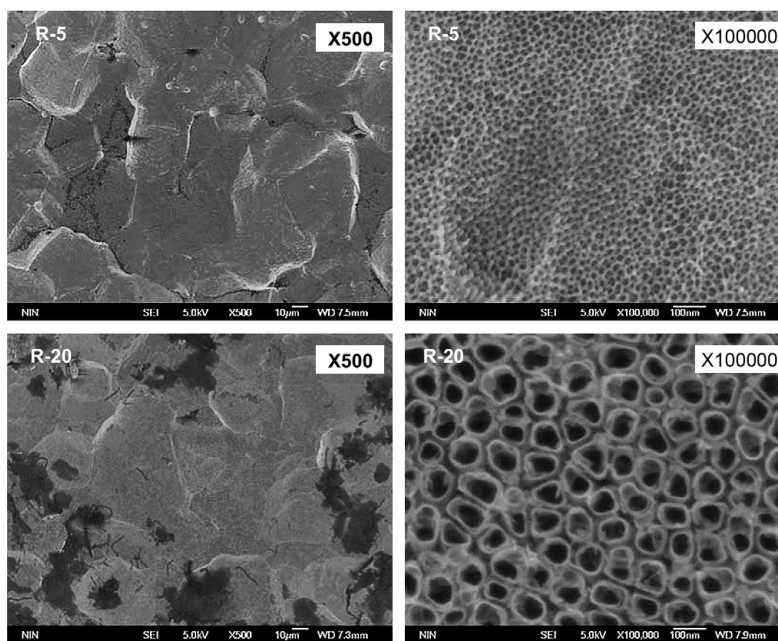


Fig. 5. SEM pictures of the hierarchical micro/nano-textured and micro titania surfaces - R-5: acid-etched/anodized at 5 V and R-20: acid-etched/anodized at 20 V. Reprinted from ref. 33, copyright (2014), with permission from Elsevier.

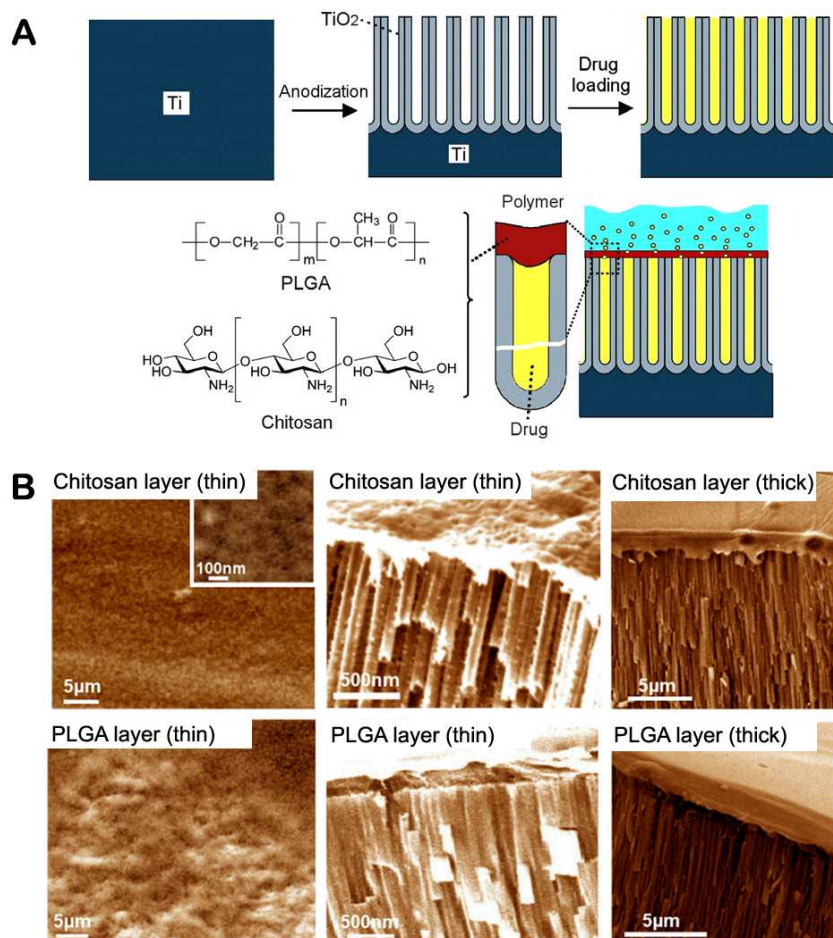


Fig. 6. (A) Schematic of titania nanotube (TNT/Ti) implants modified with polymer films. The bare TNT layer is formed on the Ti substrate by electrochemical anodization and the drug is incorporated inside the TNT structure. Finally, chitosan or a PLGA polymer film is coated on the TNT by dip coating (thin and thick) with the objective to control drug release and improve the antibacterial properties and bone integration. The schematic also shows the diffusion of drug molecules through the polymer matrix. (B) SEM images of the TNTs after drug incorporation (indomethacin) and dip coating of a polymer layer (chitosan layer and PLGA layer). Reprinted from ref. 39, copyright (2014), with permission from Elsevier.

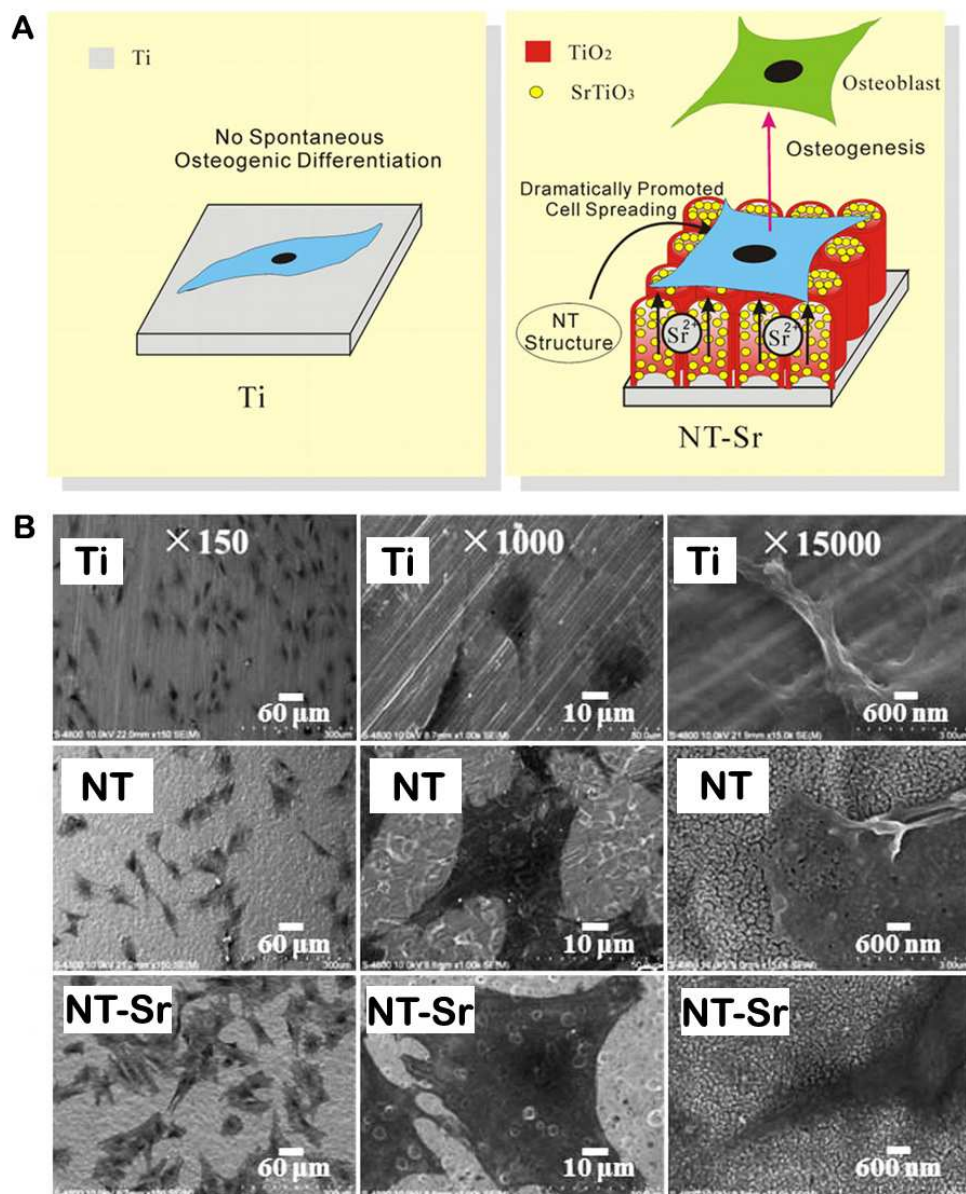


Fig. 7. (A) Schematic showing that the NT-Sr coating, combining the effect of Sr and nanomorphology of the NT, dramatically promotes MSC spreading and induces MSC selective differentiation toward osteoblasts. (B) SEM views of the cells after culturing for 2 days on Ti, NT, and NT-Sr. Reprinted from ref. 42, copyright (2014), with permission from Elsevier.

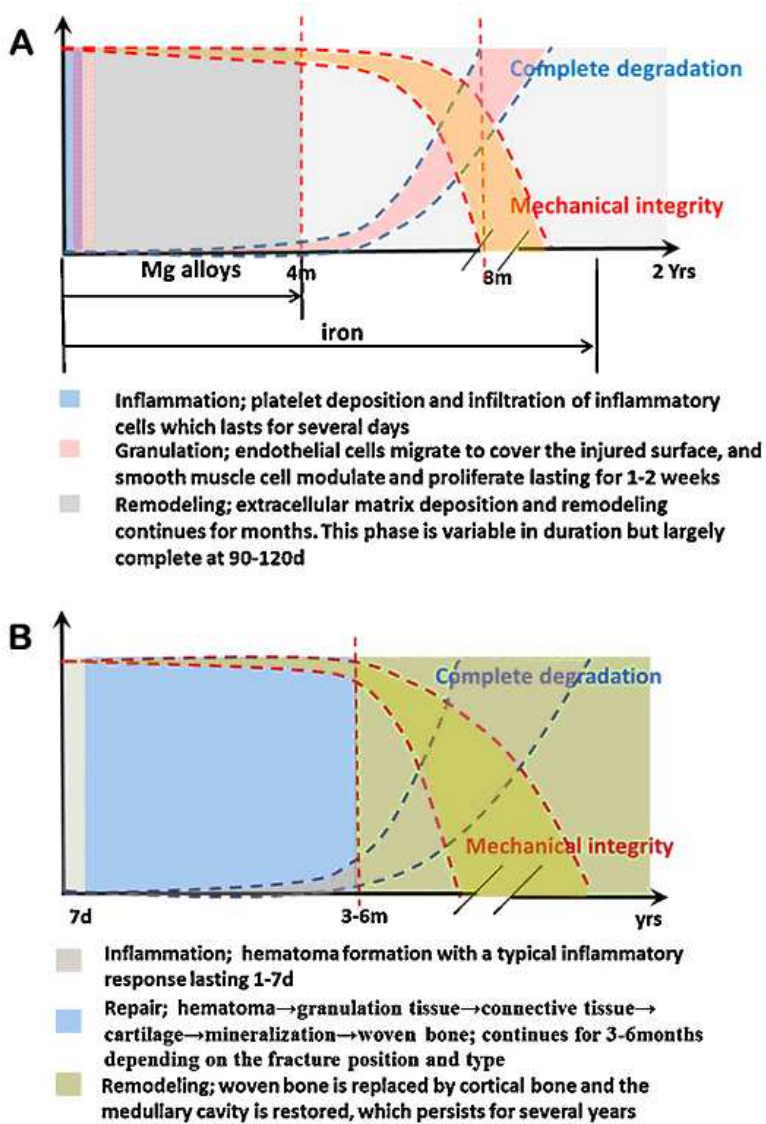


Fig. 8. (A) Schematic diagram illustrating the degradation behavior and change in the mechanical integrity of biodegradable metal (BM) stents during vascular healing. (B) Schematic diagram showing the degradation behavior and change in the mechanical integrity of biodegradable metal (BM) implants during bone healing. Reprinted from ref. 48, copyright (2014), with permission from Elsevier.

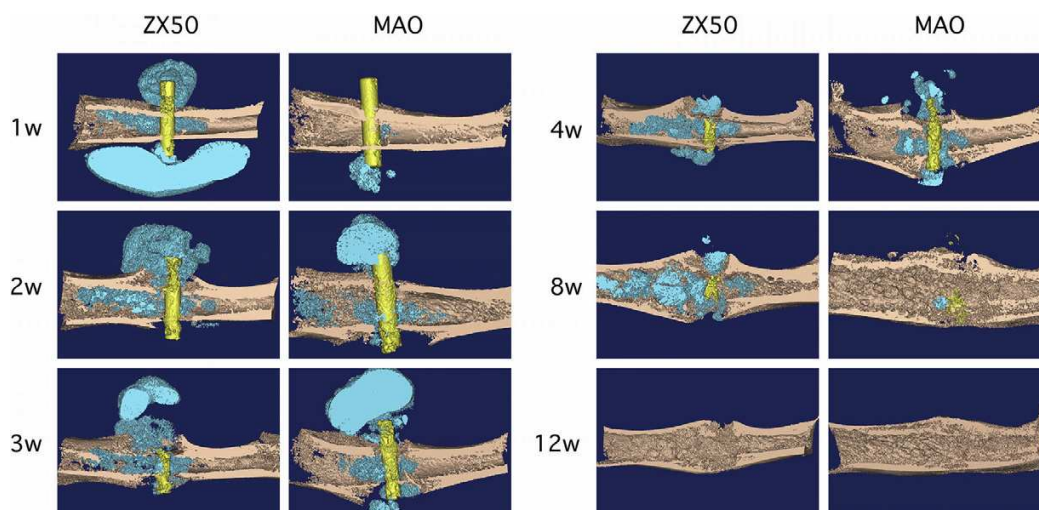


Fig. 9. μ CT Mimics[®] 3D reconstruction of the implanted site for the ZX50 and MAO implants. Gas bubbles are visible in light blue. Reprinted from ref. 66, copyright (2014), with permission from Elsevier.

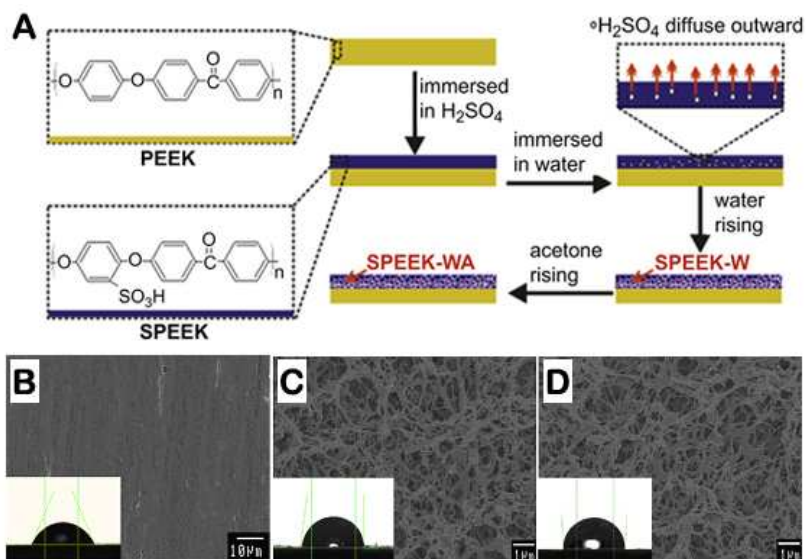


Fig. 10. (A) Schematic diagram illustrating the fabrication of the 3D porous SPEEK-W and SPEEK-WA samples. The SEM photographs are acquired from the surface of (B) PEEK control, (C) SPEEK-W, and (D) SPEEK-WA with the typical water droplet images shown at the lower left corner. Reprinted from ref. 95, copyright (2014), with permission from Elsevier.

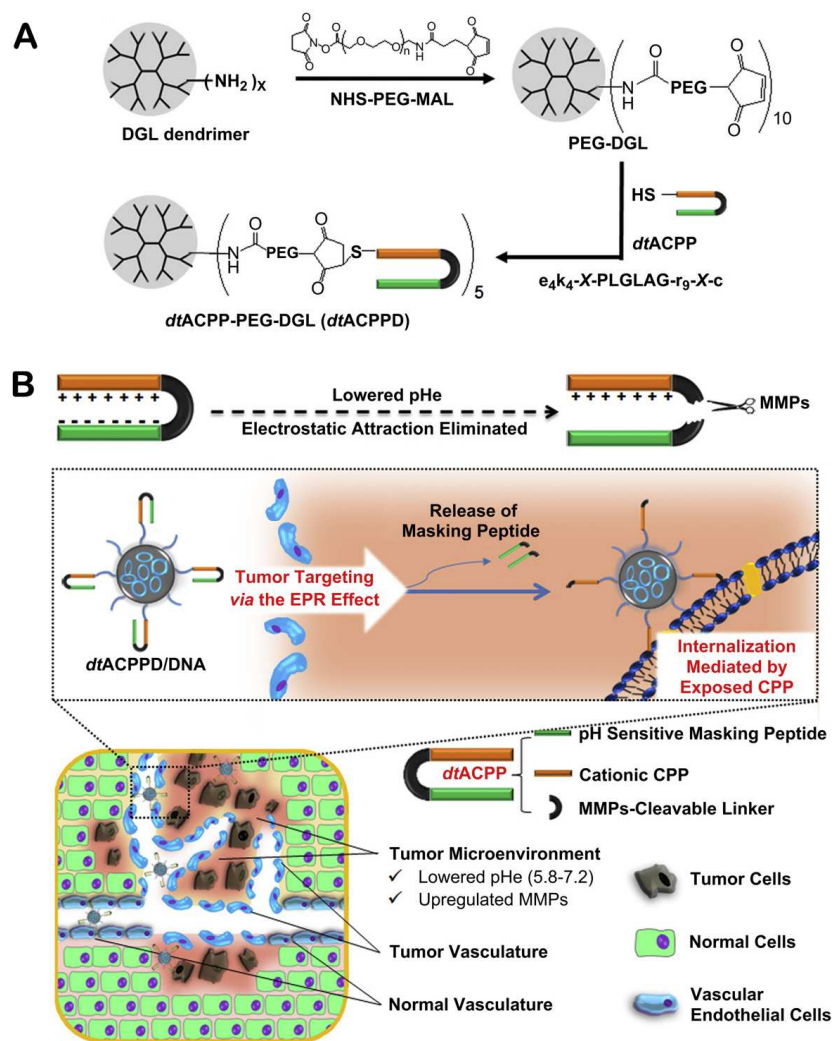


Fig. 11. (A) Synthetic steps of PEG-DGL and dtACPPD. (B) Targeting and internalization strategy of the dtACPP modified nanoparticles, dtACPPD/DNA.

Reprinted from ref. 113, copyright (2014), with permission from Elsevier.

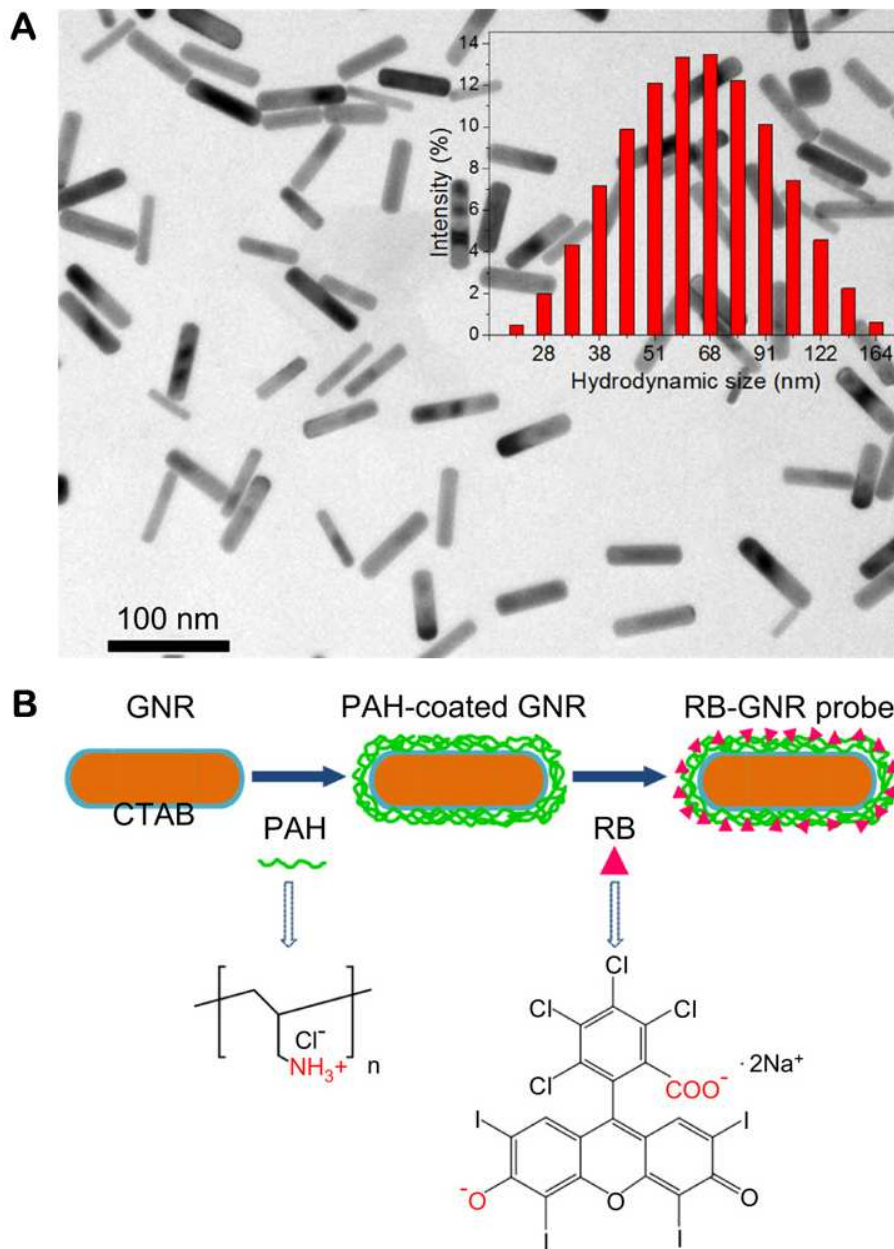


Fig. 12. (A) TEM image and hydrodynamic distribution (inset) of RB-GNRs. (B) Schematic illustration of the synthesis of RB-GNRs. Reprinted from ref. 120, copyright (2014), with permission from Elsevier.

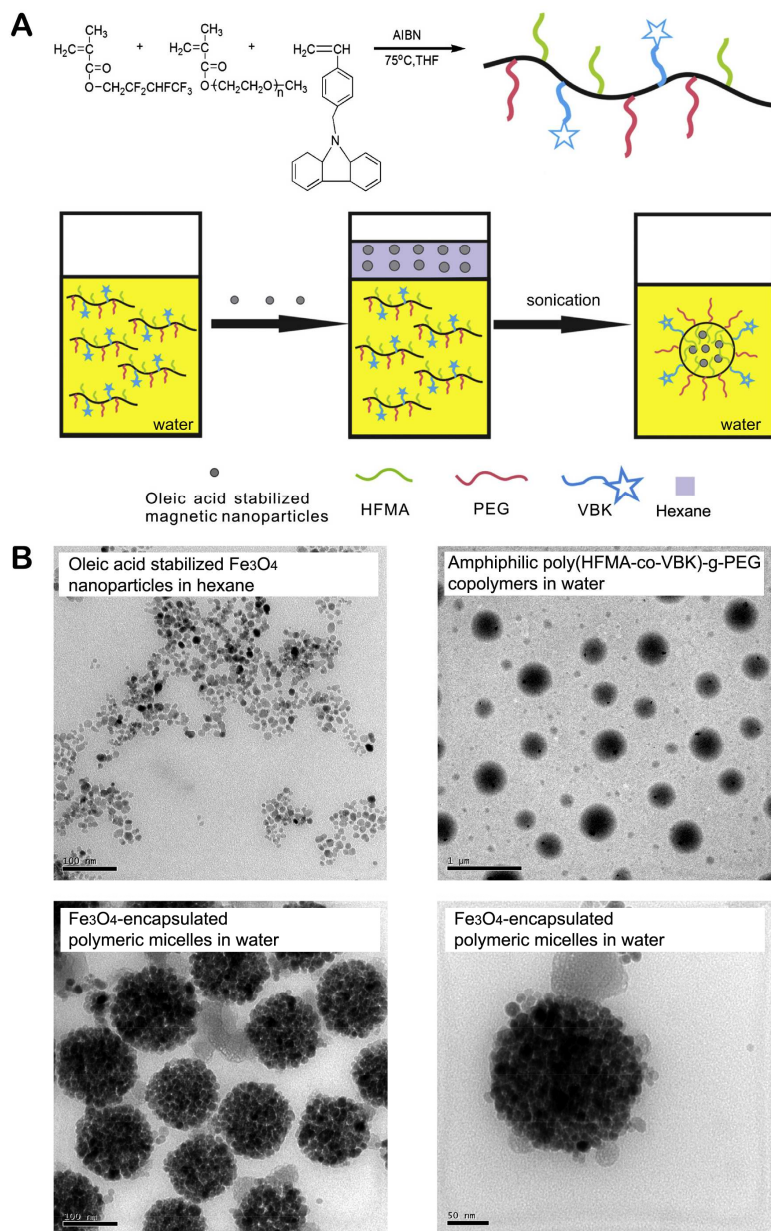


Fig. 13. (A) Schematic illustration of the preparation of magnetic fluorescent polymeric micelles encapsulated with magnetic nanoparticles by self-assembly, (B) TEM images: oleic acid stabilized Fe_3O_4 nanoparticles in hexane, amphiphilic poly(HFMA-co-VBK)-g-PEG copolymers in water, and Fe_3O_4 -encapsulated polymeric micelles in water. Reprinted from ref. 139, copyright (2014), with permission from Elsevier.

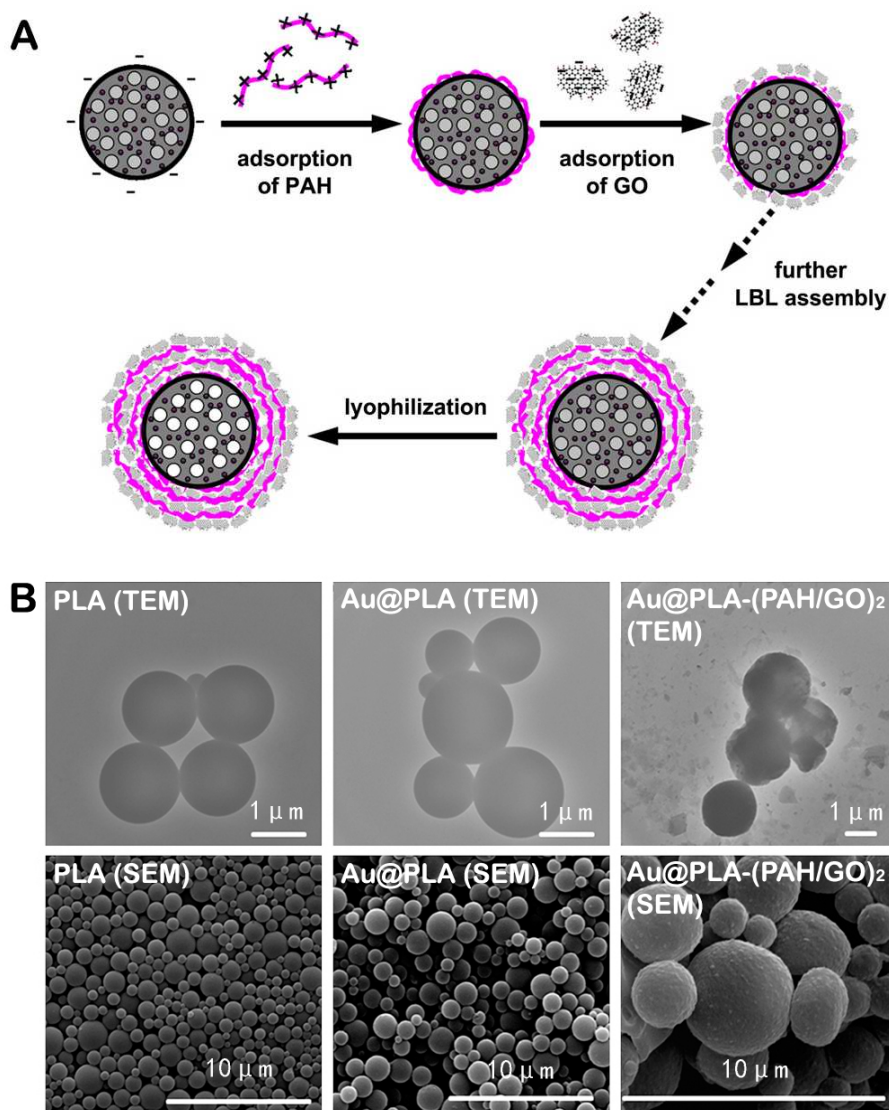


Fig. 14. (A) Illustration of the fabrication process of microcapsule of Au@PLA-(PAH/GO)_n by the layer-by-layer (LBL) technique. (B) TEM and SEM images of the microcapsules at different stages: PLA, Au@PLA, and Au@PLA-(PAH/GO)₂. Reprinted from ref. 157, copyright (2014), with permission from Elsevier.